

(NASA-TM-X-70344) BIREFRINGING ARISING  
FROM THE REORIENTATION OF THE  
POLARIZABILITY ANISOTROPY OF MOLECULES IN  
COLLISIONLESS GASES (NASA) 63 P HC  
\$6.25  
N74-35132  
Unclas  
CSCL 20H G3/24 51070

# BIREFRINGENCE ARISING FROM THE REORIENTATION OF THE POLARIZABILITY ANISOTROPY OF MOLECULES IN COLLISIONLESS GASES

C. H. Lin\*

*Ames Research Center, NASA, Moffett Field, Calif. 94035*

and

J. P. Heritage<sup>†</sup> and T. K. Gustafson<sup>‡</sup>

*Department of Electrical Engineering and  
Computer Sciences and the Electronic Research Laboratory*

*University of California, Berkeley, Calif. 94720*

R. Y. Chiao

Department of Physics

University of California, Berkeley, Calif. 94720

and

J. P. McTague<sup>§</sup>

*Department of Chemistry, University of California*

*Los Angeles, California 90024*

## ABSTRACT

The refractive index change in a collisionless gas is evaluated from the stark shifts of the rotational energy levels that arise from the polarizability anisotropy. For the limit of an extremely short-duration excitation, a multi-level coherent effect results in delayed refractive index bursts. Both stationary and transient responses of this birefringence to an optical field are considered for symmetric top molecules, with particular emphasis on the special case of linear molecules.

## I. INTRODUCTION

The birefringence induced by a uniform electromagnetic field in a fluid composed of anisotropic molecules arises primarily from the reorientation of

the molecules due to their interaction with the field through the molecular electric dipole moment<sup>1</sup> and the anisotropy of the static polarizability.<sup>2</sup> The present work is restricted to the rotational response of polar and non-polar molecules excited by short optical pulses for which the interaction is primarily through the polarizability anisotropy. Though the permanent dipole interaction dominates for frequencies of the applied field ranging from dc to microwave, at higher frequencies it plays a diminishing role. In liquids, this rolloff of the rotational response with increasing frequency results from a damping of the rotational motion due to viscous interaction with neighboring molecules. For gases, collisional or inertial effects are responsible for such a rolloff. Consequently, for both liquids and gases, at optical frequencies the interaction through the permanent dipole moment is extremely weak.

Molecular reorientation resulting from the interaction through the polarizability anisotropy depends on the square of the electric field, so that even for optical frequencies there are low-frequency components that produce a significant rotational response<sup>2</sup> and hence induced birefringence. This nonlinear optical birefringence has been treated for liquids by a generalization of Debye's classical theory of molecular rotation.<sup>1,3</sup> The result shows that the angular distribution of the molecules achieves thermodynamic equilibrium in a characteristic time that is 1/3 the viscous relaxation time deduced by Debye for polar molecules. This characteristic time, typically of the order of tens of picoseconds, is much larger than the mean time between molecular collisions (collision time).

In gases for which the collision time is much greater than the rotational period of the molecules, quantization of the rotational motion is important. Nevertheless, when the gas interacts with a smooth light pulse having a duration much longer than the collision time, thermodynamic equilibrium

is maintained just as in liquids. For this case, the classical thermodynamic approach employed by Bloembergen and Lallemand<sup>3</sup> is a good approximation.

The primary concern of this paper is in the nonequilibrium situation, i.e., birefringence in gases induced by optical disturbances shorter than the collision time. The gas is thus considered to be "collisionless," and the momentum associated with the molecular rotation must be considered explicitly.

We first deduce a nonequilibrium induced refractive index change for linear molecules from the quartic and higher order Stark shifts of the rotational energy levels evaluated from time-independent perturbation theory. Such an approach is strictly valid for an interaction with optical pulses which, although less than the collision time in duration, are longer than the inverse of the fundamental rotational transition frequency. However, even for a much shorter excitation, the transient response of the gas during the excitation is in many cases of experimental interest quite well approximated by this stationary theory. The lowest order nonlinear refractive index change which is directly proportional to the square of the electric field intensity is tabulated for several gases composed of linear molecules or symmetric top molecules. These range from  $4 \times 10^{-13} \text{ (stat volt/cm)}^{-2} \text{ (mole/cm}^3\text{)}^{-1}$  for  $\text{H}_2$  at  $35^\circ \text{ K}$  to  $2 \times 10^{-10} \text{ (stat volt/cm)}^{-2} \text{ (mole/cm}^3\text{)}^{-1}$  for  $\text{CS}_2$  at  $320^\circ \text{ K}$ . Analytic expressions for the refractive index change in both the high-temperature limit and the low-temperature limit are given. Saturation of this refractive index change for high field intensity is also discussed.

When the optical pulses are shorter than both the collision time and the inverse of the fundamental quadrupole transition frequency, the molecular rotational response cannot follow the excitation instantaneously. Hence the refractive index change has an explicit time-dependence and can persist subsequent to excitation. For such an ultra-short excitation, the refractive index change is

deduced from the density matrix equations for the molecular rotation. For a gas composed of linear molecules, it has already been shown<sup>4</sup> that after excitation with a single light pulse a periodic recurrence of the birefringence should result. These recurrences, which are due to quantum interference, can have an extremely short duration since many rotational levels can contribute. The individual echoic bursts should be separated by a time given by  $1/4Bc$ , where  $B$  is the rotational constant of the molecules in wave numbers and eventually should decay away due to collisional and Doppler effects.

In the present paper, this explicitly time-dependent refractive index change has been investigated more extensively. In particular, we consider the transient refractive index change during the presence of the optical excitation which in many situations is approximated well by the stationary results. The influence of the excitation pulse width, the molecular rotational constant, and the gas temperature on the amplitude and the duration of the refractive index bursts is also considered in detail. In addition, the results are generalized to include symmetric top molecules.

The paper is divided into seven sections. In the following section, the Hamiltonian describing the interaction between molecules possessing a linear but anisotropic polarizability, and an optical field is considered. In section III the time-independent perturbation calculation of the quartic and higher order Stark shifts of the rotational energy levels of linear molecules is given and the induced refractive index change for a gas composed of such molecules is determined. In § IV a general expression for the lowest order time-dependent non-linear refractive index change for gases composed of symmetric top molecules is derived from the density matrix representation of the rotational states. In § V, we determine the stationary refractive index change for symmetric top molecules as a limit of the time-dependent expression obtained in § IV and compare

this result with that for a linear molecular gas. In § VI, the time-dependent behavior of symmetric top molecules is investigated and the special case of linear molecules is discussed in detail. In the final section, the possibility of detecting the echoic refractive index bursts, its application, and integral properties of the time-dependent refractive index change are discussed.

## II. THE PERTURBATION HAMILTONIAN FOR LINEAR POLARIZABLE MOLECULES

In this section, we define the Hamiltonian that describes the interaction between the rotational energy levels of linear molecules with an electric field oscillating at optical frequencies. The interaction is assumed to arise through the anisotropic polarizability and the optical intensity which is, in general, time-varying.

Linear molecules are particularly easy to treat since the polarizability is characterized by only two components -  $\alpha_{\parallel}$ , the polarizability along the molecular axis, and  $\alpha_{\perp}$ , that perpendicular to the molecular axis. The change in the potential energy of the rotational states produced by the interaction of the molecules with the radiation field is a function of  $\Delta\alpha = \alpha_{\parallel} - \alpha_{\perp}$ , the anisotropy, and  $\theta$ , the angle between the molecular symmetry axis and some fixed direction in space. The latter is chosen to be the direction of the component of the angular momentum which commutes with the square of the magnitude of the total angular momentum vector.

For a linearly polarized optical field propagating in the z-direction, the electric field is written in the form:

$$\vec{E} = \left\{ \frac{E_0(t,z)}{2} \exp[i(\omega t - kz)] + \text{c.c.} \right\} \hat{a}_x \quad (1)$$

where  $\hat{a}_x$  is a unit vector specifying the polarization direction of the field and c.c. represents the complex conjugate of the first term. In this case,  $\hat{a}_x$

is chosen as the projection axis for the commuting component of the angular momentum vector.  $E_0(t, z)$ , the electric-field amplitude is assumed to vary slowly in time ( $\partial E_0 / \partial t \ll \omega$ ) and in space ( $\partial E_0 / \partial z \ll k$ ). In all cases, the reaction of the medium on the field is neglected. Consequently,  $E_0(t, z) \approx E_0[t - k/\omega z]$ , where the propagation constant  $k$  is equal to  $\omega/c$ ,  $c$  being the speed of light in the gas.

The perturbing Hamiltonian for such a linearly polarized field is

$$H' = -\frac{1}{2} \Delta \alpha \langle \vec{E} \cdot \vec{E} \rangle \cos^2 \theta - \frac{1}{2} \alpha_{\perp} \langle \vec{E} \cdot \vec{E} \rangle \quad (2)$$

in which  $\langle \vec{E} \cdot \vec{E} \rangle$  is the average over an optical cycle of the square of the electric field amplitude or  $E_0(t, z)E_0^*(t, z)/2$ . Such an average results since only the low-frequency term proportional to the time-averaged intensity of the electric field can appreciably perturb the molecular rotational energy states. The angular response of the molecules to the torque at frequency  $2\omega$  of  $\langle \vec{E} \cdot \vec{E} \rangle$  is extremely weak because of molecular inertia.

If the optical pulse is circularly polarized and propagating in the  $z$ -direction, the plane containing the electric field vector is defined by the mutually orthogonal unit vectors  $\hat{a}_x$  and  $\hat{a}_y$ . The electric field vector can be written in the form

$$\vec{E} = \frac{E_0(t, z)}{2\sqrt{2}} \left[ e^{i(\omega t - kz)} (\hat{a}_x + i\hat{a}_y) + \text{c.c.} \right] \quad (3)$$

For this polarization, the direction of propagation  $\hat{a}_z$  is also chosen as the direction of the commuting component of the angular momentum. The perturbation Hamiltonian, for this case, is

$$H' = -\frac{1}{4} \Delta \alpha \langle \vec{E} \cdot \vec{E} \rangle \sin^2 \theta - \frac{1}{2} \alpha_{\perp} \langle \vec{E} \cdot \vec{E} \rangle \quad (4)$$

### III. STATIONARY REFRACTIVE INDEX CHANGE FOR GASES COMPOSED OF LINEAR MOLECULES

In many of the experiments anticipated, the intensity of the optical excitation is expected to vary negligibly for times much shorter than the period determined by the transitions between the most highly populated rotational levels of the molecule. The refractive index change induced during excitation with the optical pulse is then dependent primarily on the electric-field intensity and not explicitly on time. A stationary solution of the Schroedinger equation is quite adequate for this portion of the response. This considerably simplifies the calculation and allows a simple estimate of the refractive index response for particular molecular gases. The influence of saturation due to a high laser field intensity is also more easily treated in the absence of an explicit time dependence.

The intensity dependent optical index of refraction  $n = n_0 + n_2 \langle \vec{E} \cdot \vec{E} \rangle + n_4 \langle \vec{E} \cdot \vec{E} \rangle^2 + n_6 \langle \vec{E} \cdot \vec{E} \rangle^3$  can be obtained from the energy change,  $\Delta W$  induced by the presence of the electric field. Since  $4\pi N \frac{\partial \Delta W}{\partial \langle \vec{E} \cdot \vec{E} \rangle}$  is the susceptibility, where

$$N \text{ is the number density, } \frac{1}{2}$$

$$n = \left[ 1 - 4\pi N \frac{\partial \Delta W}{\partial \langle \vec{E} \cdot \vec{E} \rangle} \right]^{\frac{1}{2}}$$

(5)

$$\approx n_0 + (1 - n_0 - 4\pi N \frac{\partial \Delta W}{\partial \langle \vec{E} \cdot \vec{E} \rangle}) / (2n_0)$$

assuming a dilute gas. The energy change  $\Delta W$  is obtained from the Stark shifts of the rotational energy levels of the molecules.

There are two limiting situations which should be distinguished. The first occurs for optical pulses much longer than the collision time. The presence of collisions assures that the population distribution of the Stark shifted energy levels is Boltzmann - labeled the thermodynamic equilibrium case. In Appendix B, it is shown that both the quadratic and the quartic Stark shifts contribute

to the coefficient  $n_2$ , which to a good approximation is given by the usual classical expression<sup>3</sup>:

$$\frac{4\pi N}{45} \frac{(\Delta\alpha)^2}{kTn_0}$$

The second case is based on an absence of molecular collisions and thus is valid for optical pulses much shorter than the mean collision time. For this case, which is the primary concern of the present paper, the population of each shifted rotational level is frozen to the value determined by the initial zero field Boltzmann distribution. The total energy change due to the Stark shifts is then

$$\Delta W = \frac{\sum_{J=0}^{\infty} \sum_{M=-J}^{+J} E_{J,M} e^{-(E_{J,M}^{(0)}/kT)}}{Z} \quad (6)$$

where  $E_{J,M}^{(0)}$  is the unperturbed rotational energy eigenvalue corresponding to a particular angular quantum number  $J$  and its projection  $M$  along the chosen fixed axis.  $Z$  is the partition function  $\sum_{J=0}^{\infty} (2J+1) e^{-E_{J,M}^{(0)}/kT}$ , and  $n = \frac{hBc}{kT}$ .  $E_{J,M}$  is the perturbed rotational energy eigenvalue corresponding to the unperturbed Hamiltonian plus the interaction Hamiltonian of Eq. (2) or (4).

The appropriate solutions of the time-independent Schroedinger equation for the Hamiltonian of Eq. (2) or Eq. (4) are the spheroidal wave functions.<sup>5</sup> Calculation of the corresponding perturbed rotational energy eigenvalue  $E_{J,M}$  presents severe difficulties and has not been expressed analytically for an arbitrary field strength. The usual perturbation expansion, which is useful when the electric field is weak, is expressed as

$$E_{J,M} = hBc(\lambda_0 + K\lambda_1 + K^2\lambda_2 + \dots) - \frac{1}{2} \alpha_{\perp} \langle \vec{E} \cdot \vec{E} \rangle \quad (7)$$



with K the perturbation expansion parameter,  $1/2 \Delta\alpha \langle \vec{E} \cdot \vec{E} \rangle / hBc$  and  $\lambda_0 hBc$  is the unperturbed energy eigenvalue  $J(J+1) hBc$ . Values for  $\lambda_1, \lambda_2, \lambda_3, \dots$  in terms of increasing numbers of algebraic terms, as obtained from the standard perturbation approach are tabulated in Ref. (5). These can only be used as a starting point for the refractive index calculation. Considerable effort is involved in combining the factors and in simplifying the resultant expressions.

If Eq. (7) is substituted into Eq. (6),  $\Delta W$  for the collisionless case can be expressed as

$$\langle \Delta W \rangle = \frac{hBc \sum_i N_i(\eta) K^i}{Z\eta} \quad (8)$$

where the sums  $N_i(\eta) = \sum_{J=0}^{\infty} \sum_{M=-J}^J \lambda_i e^{-J(J+1)\eta}$ , and  $\eta = \frac{hBc}{kT}$ .

The first three coefficients in the nonlinear refractive index expression, obtained from Eqs. (8) and (6) are

$$n_2 = -\frac{2\pi N}{kT n_0} N_2(\eta) \Delta\alpha^2 / Z\eta \quad (9a)$$

$$n_4 = -\frac{3\pi N}{2kThBcn_0} N_3(\eta) \Delta\alpha^3 / Z\eta \quad (9b)$$

$$n_6 = -\frac{4\pi N}{kT(hBc)^2 n_0} N_4(\eta) \Delta\alpha^4 / Z\eta \quad (9c)$$

Considerable simplification occurs if sum rules over the projection quantum number M for the coefficients  $\lambda_i$  of the various orders in the perturbation expansion can be obtained. We thus wish to consider the pertinent aspects of the perturbation theory more deeply and in particular to outline the calculation of these.

For this, the collisionless case, the nonlinear refractive index change is independent of the quadratic Stark shift  $hB\lambda_1 K$ . However as pointed out earlier and in Appendix B this can contribute to the coefficient  $n_2$  after collisions have significantly thermalized the population among the perturbed states.

For both linear and circular polarization the quadratic shifts, which respectively are<sup>6,7</sup>

$$\Delta W_1 = K\lambda_1 hBc = -\frac{1}{2} \Delta\alpha \langle \vec{E} \cdot \vec{E} \rangle \frac{2J(J+1) - 2M^2 - 1}{(2J-1)(2J+3)} \quad (10a)$$

$$\Delta W_1 = -\frac{1}{4} \Delta\alpha \langle \vec{E} \cdot \vec{E} \rangle \frac{2J(J+1) + 2M^2 - 2}{(2J-1)(2J+3)} \quad (10b)$$

indicate that each rotational level is shifted down in energy in the presence of an optical field (Figs. (1) (2)) since the induced molecular polarization in the direction of the field for a molecule in any state is positive. Furthermore, the average of this negative quadratic Stark shift, over the quantum number  $M$  of the rotational sublevels, is independent of the rotational level quantum number  $J$  since the sum rule  $\sum_{M=-J}^{+J} \lambda_1 = -\frac{1}{3} J(2J+1)(J+1)$  is valid. Thus each level ( $J$ ) contributes equally to the macroscopic linear polarizability  $(\alpha_{||} + 2\alpha_{\perp})/3$  per molecule.

This decrease in rotational energy indicated by the quadratic Stark shift is quite in contrast with that which results from a permanent dipole interacting with a low-frequency field, which for comparison is displayed to the left of Fig. (1). In its rotational ground state, the permanent dipole moment tends to align along the direction of the applied electric field and the interaction energy is negative. On the other hand, in states for which  $M = 0$ ,  $J \neq 0$ , the permanent dipole moments spend more time oriented in opposition to the electric field; hence the interaction energy is greater than zero and the energy levels are shifted up. For states with  $M \neq 0$  in addition to this, a component of the torque is

present which tends to align the molecules along the direction of the electric field. Hence, the levels can be shifted either up or down. As a result aside from the ground state, the energy of each rotational level  $J$  averaged over the quantum number  $M$  is not changed due to the quadratic Stark shift. Consequently, the influence of the permanent dipole moment on the linear polarization of a gas in thermodynamic equilibrium arises entirely from the ground state.<sup>1</sup>

Obtaining the nonlinear collisionless refractive index coefficient  $n_2$  of Eq. (9a) necessitates a calculation of the third term in Eq. (7)  $hBc\lambda_2 K^2$  which is the quartic Stark shift in rotational energy. The perturbation result consists of two contributions which arise from a coupling of the  $J, M$  rotational energy level to the two neighboring rotational states satisfying  $\Delta J = \pm 2$ ,  $\Delta M = 0$ , as determined by the selection rules for the  $\cos^2 \theta$  dependence of the induced dipole moment. This contribution to the induced energy shift of the rotational state  $J, M$  can be interpreted as a mutual repulsion of these coupled states. After carrying out the tedious algebraic multiplication and factorization required to combine and simplify the two separate terms given in Ref. (5) one can express the quartic shift as

$$\Delta W_2 = hBcK^2 \lambda_2 = hBcK^2 \frac{M^4 P(J) - M^2 Q(J) + R(J)}{(2J-3)(2J-1)^3(2J+1)(2J+3)^3(2J+5)} \quad (11)$$

where

$$P(J) = 80J^3 + 120J^2 + 172J + 66$$

$$Q(J) = 96J^5 + 240J^4 + 88J^3 - 108J^2 + 68J + 60$$

$$R(J) = 16J^7 + 56J^6 + 12J^5 - 110J^4 - 44J^3 + 72J^2 + 22J - 6$$

This is the most important term in the series expansion of the energy shift due to the optical field. In Fig. (2), in which the energy levels of several of the lower rotational states are plotted as a function of the perturbation parameter  $K$ , the curvature near  $K = 0$  gives the quartic Stark shift. This can be either positive or negative depending upon the particular energy state.

Although a relatively complicated expression, the sum of the quartic Stark shifts over the projected quantum number  $M$ , which enters into the most important nonlinear coefficient  $n_2$ , is particularly simple. This can be conveniently obtained from Eq. (8) and is expressed as

$$F_2(J) = \sum_{M=-J}^J \lambda_2 = -\frac{1}{60} \left[ \frac{1}{(2J-1)^2} - \frac{1}{(2J+3)^2} \right] \quad (12)$$

Higher order terms in the perturbation expansion are necessary to describe the rotational energy level shifts for optical intensities such that  $K \gg 1$ . Computer multiplication and factorization programs were employed to express the next two orders,  $\lambda_3$  and  $\lambda_4$ , in the form included in Appendix A, which is convenient for deducing the sum rules. It will be apparent that many more terms are required for an adequate description of such a saturated case, except for the low-temperature limit when only the ground state is significantly populated. This presents major computational difficulties which have not been pursued.

$\lambda_3$  and  $\lambda_4$  considerably simplify when the sums over  $M$  are taken. If the results are expanded as a partial fraction expansion one obtains

$$F_3(J) = \sum_{M=-J}^J \lambda_3 = \frac{1}{210} \left[ \frac{1}{(2J-1)^2} - \frac{1}{(2J+3)^2} - \frac{1}{(2J-1)^4} + \frac{1}{(2J+3)^4} \right] \quad (13)$$

$$\begin{aligned}
F_4(J) = \sum_{M=-J}^J \lambda_4 = \frac{1}{5040} & \left[ \frac{9}{16(2J-1)^2} - \frac{9}{16(2J+3)^2} \right. \\
& + \frac{59}{4(2J-1)^4} - \frac{59}{4(2J+3)^4} - \frac{15}{(2J-1)^6} \\
& \left. + \frac{15}{(2J+3)^6} - \frac{9}{32(2J-3)^2} + \frac{9}{32(J+5)^2} \right] \quad (14)
\end{aligned}$$

Using the sum rules, Eqs. (12) to (14), the sums  $N_i(\eta)$  in Eq. (8) can be handled with relative simplicity, at least numerically. Calculations of  $N_2(\eta)$ ,  $N_3(\eta)$ , and  $N_4(\eta)$  are shown as functions of  $\eta$  in Fig. 3, along with the factor  $Z\eta$ .

Particularly simple analytical expressions can be obtained for  $n_2$ ,  $n_4$ , and  $n_6$  in the low temperature limit ( $\eta > 2$ ). The nonlinearity in the refractive index is then determined solely by the Stark shift of the ground state and the coefficients of the refractive index change are approximately equal to

$$n_2 = \frac{4\pi N}{135} \frac{(\Delta\alpha)^2}{\hbar Bc n_0} \quad (15a)$$

$$n_4 = \frac{6\pi N}{8505} \frac{(\Delta\alpha)^3}{(\hbar Bc)^2 n_0} \quad (15b)$$

$$n_6 = -\frac{13\pi N}{1913625} \frac{(\Delta\alpha)^4}{(\hbar Bc)^3 n_0} \quad (15c)$$

Since  $n_6$  is negative, the saturation of the refractive index with an increasing optical field intensity is well approximated by these three coefficients as illustrated in Fig. 4. The saturated value of 4.9 at  $K \approx 50$  is close to the expected value for complete alignment in the direction of the field, which is 4.2.

The other extreme, that of the high temperature limit ( $\eta < 0.01$ ) is applicable to many molecular gases at room temperature (for  $\text{CS}_2$  at  $T = 300^\circ \text{K}$ ,  $\eta \approx 5 \times 10^{-4}$ ). In this limit,  $Z\eta \approx 1$  and  $N_2(\eta)$  can then be approximated by

$\sum_{J=0}^{\infty} \sum_{M=-J}^J \lambda_2$  which from Eq. (12) is  $-1/30$ . Thus

$$n_2 = \frac{2\pi N}{30} \frac{\Delta\alpha^2}{kTn_0} \quad (16)$$

This value of  $n_2$ , which arises entirely from the quartic Stark shifts, is a factor of  $3/4$  smaller than the usual thermal equilibrium value,<sup>3</sup> which has contributions from the quadratic shift as well (Appendix B).

The similarity of this expression to the thermal equilibrium expression and in particular to the lack of dependence on the quantized behavior of the gas suggests that Eq. (16) is, in principle, derivable from a classical description of the molecular interaction with the field. This calculation appears to be extremely difficult since the absence of thermodynamic equilibrium implies that the nonlinear equations of motion for each molecule would have to be solved explicitly and an orientational average then taken.

Useful analytical expressions for  $n_4$  and  $n_6$  are much more difficult to obtain in the high temperature limit. From Eqs. (13) and (14) the sums of the sixth and eighth order Stark shifts over all the levels are both zero since  $\sum_{J=0}^{\infty} F_3(J)$  and  $\sum_{J=0}^{\infty} F_4(J)$  are both equal to zero. This is also apparent from Fig. (3).

Thus in contrast to the case of  $n_2$ , for which the Boltzmann factor could be assumed equal to 1 for all terms in  $N_2(\eta)$  the deviation of the Boltzmann factor from unity in  $N_3(\eta)$  and  $N_4(\eta)$  must be considered in order to obtain analytical expressions for  $n_3$  and  $n_4$ . Expansion of the Boltzmann factor in terms of  $\eta$  results in divergent series in the sums over  $J$  and hence is not useful. Due

to the compensating Stark shifts however, without additional higher order coefficients the terms  $n_4$  and  $n_6$  do not specify the saturated behavior. Hence we shall not pursue these problems further.

With regards to a more accurate description of the refractive index saturation one might consider a numerical calculation the Stark shifted energy eigenvalues for a strong perturbation. Such calculations have been attempted. However these have been restricted to rotational levels for  $J \leq 10$  which is insufficient for an evaluation of the nonlinear refractive index.

Stern<sup>8</sup> obtained numerical solutions for the energy levels by solving for the roots of an implicit continued fraction expansion of the energy eigenvalues. However, these roots are also extremely difficult to determine for large values of the perturbation parameter ( $K \gg 20$ ). These results have been extended by Curl et al.<sup>9</sup> by combining a numerical diagonalization of the approximated Hamiltonian matrix with the results of the continued fraction expression. In this manner, they are able to evaluate the perturbed energy for some lower energy levels for values of  $K$  up to 500.

The Stark shifts for a few rotational energy levels obtained both by the power series approximation including perturbation terms up to  $\lambda_4$  and numerically by Curl et al. are plotted in Fig. 2. For  $K \leq 10$ , for which the power series is quite close to the results obtained numerically, the motion of molecules can be described as "rotational." As the perturbing energy is increased, however, the molecular rotation is hindered and eventually the motion is more properly described as "oscillatory."<sup>10</sup> Groups of energy levels merge, each group being characterized by a librational quantum number. (This behavior is indicated on the right-hand side of Fig. 2.) It is apparent that the limiting value of the refractive index is that obtained by total alignment of molecules,  $n = 1 + 2\pi N\alpha_{||}$ . This is

indicated directly in Fig. 2 since the slope of the energy levels asymptotically approach -1 for extremely high electric-field intensity.

The most important coefficient to consider experimentally is  $n_2$  since it provides the strength of the various possible nonlinear interactions. This coefficient is given in Table 1 for several gases of potential interest. For  $\text{CO}_2$ ,  $\text{CS}_2$ ,  $\text{C}_2\text{H}_2$  and  $\text{N}_2\text{O}$ ,  $n_2$  is well approximated by Eq. (16) at  $300^\circ\text{K}$ .

The coefficient for hydrogen at  $35^\circ\text{K}$  and deuterium at  $40^\circ\text{K}$  can be approximated by the low-temperature limit if thermal equilibrium is assumed. Nuclear statistics have been taken into account in the calculation for  $\text{N}_2$  and  $\text{O}_2$ <sup>(11)</sup>. Even though these two molecules have relatively small moments of inertia, the results do not differ appreciably from those evaluated from Eq. (5). The index coefficients for  $\text{HCl}$  and  $\text{HBr}$  vapors at room temperature were determined by using  $\text{N}_2(n)$  and  $\text{Zn}$  from Fig. 3 in conjunction with Eq. (9).<sup>12</sup>

#### IV. FIRST ORDER DENSITY MATRIX CALCULATION OF TIME-DEPENDENT REFRACTIVE INDEX CHANGES OF GASES COMPOSED OF SYMMETRIC TOP MOLECULES

In many cases pulsed optical or infrared excitation of vapors composed of anisotropically polarizable molecules will produce a refractive index change which is quite well described by the stationary results during the excitation. In addition to this adiabatic portion of the response, however, quantum mechanical interference occurs. This is appreciable if the frequency spectrum of the pulse intensity overlaps many rotational transitions and results in an index of refraction subsequent to the excitation. For many di- and tri-atomic molecular vapors excited by pulses typical of the mode locked glass laser an intermediate regime in which both the adiabatic and quantum interference effects are present is expected.

In the present section we wish to introduce two generalizations of the previous results to treat the experimentally expected behavior for a variety of vapors. Firstly, the time dependence in the nonlinear refractive index change will be



treated by utilizing the density matrix equations for the rotational motion. The calculation will, however, only be carried out for the lowest order in the optical intensity so that saturation will not be considered. Secondly, the rotational inertia along the figure axis as well as that perpendicular to the figure axis will be considered to include the more general class of symmetric top molecules. This additional inertia is expressed through additional terms in the unperturbed Hamiltonian. As for the special case of linear molecules, the polarizability is still specified by two components -  $\alpha_{||}$ , parallel to the figure axis and  $\alpha_{\perp}$ , perpendicular to the figure axis. As a result, the directionally-dependent, perturbing Hamiltonian is the same as for linear molecules.

In section V the stationary limit of the general time dependent susceptibility change is obtained. This will provide  $n_2$  for symmetric molecules. The presence of the additional states as specified by the quantized component  $\hbar \Lambda$  along the figure axis considerably complicates the perturbation calculation for the stationary Stark shifts. Although the quartic Stark shifts are obtained relatively easily, terms of any higher order are extremely cumbersome. In addition, numerical calculations of the highly perturbed rotational states have apparently not been attempted thus far.

In section VI we specialize the discussion to the temporal development of the quantum interference exhibited by the collection of evolving superposition states induced by a sufficiently short excitation.

To proceed with the calculation of the refractive index change for symmetric top molecules we denote the element of the density matrix between two rotational states specified by the quantum numbers  $I, M, \Lambda$  and  $J, M, \Lambda$  by  $\rho_{I,J}$ . In analogy to linear molecular gases, the quantum numbers  $M$  and  $\Lambda$  need not be considered explicitly. However, it must be kept in mind that whenever a sum arises it is to be taken over  $M$  and  $\Lambda$  as well as  $J$ .

The equations of motion for the density matrix are<sup>13</sup>

$$\frac{\partial \rho_{I,J}}{\partial t} = \frac{i}{\hbar} \sum_K (\rho_{I,K} H_{K,J} - H_{I,K} \rho_{K,J}) \quad (17)$$

where  $H = H^0 + H'$  is the total Hamiltonian,  $H'$  being specified by expression (2) or (4), depending on the polarization. From this point on, we will specifically discuss linear polarization.

The matrix elements of  $H^0$ , the unperturbed energy eigenvalues, are<sup>6,11</sup>

$$H_{J,\Lambda}^0 = hBcJ(J+1) + hc(A - B)\Lambda^2 \quad (18)$$

where  $A$  and  $B$  are, respectively, the rotational constant about the figure axis and that about the axis perpendicular to the figure axis.

The matrix elements of the perturbing Hamiltonian are

$H'_{I,J} = -1/2 \Delta\alpha \langle \vec{E} \cdot \vec{E} \rangle Q_{I,J}$ . The  $Q_{I,J}$ , which are the matrix elements for the operator  $\cos^2\theta$ , can be obtained by using the table given by Cross *et al.*<sup>14</sup> These matrix elements are

$$Q_{J,J-2} = \frac{1}{J(J-1)(2J-1)} \left\{ \frac{(J^2-M^2)(J^2-\Lambda^2)[(J-1)^2-M^2][(J-1)^2-\Lambda^2]}{(2J-3)(2J+1)} \right\}^{1/2} \quad (19a)$$

$$Q_{J,J+2} = \frac{1}{(J+1)(J+2)(2J+3)} \left\{ \frac{[(J+2)^2-M^2][(J+2)^2-\Lambda^2][(J+1)^2-M^2][(J+1)^2-\Lambda^2]}{(2J+1)(2J+5)} \right\}^{1/2} \quad (19b)$$

$$Q_{J,J} = \frac{(J^2-M^2)(J^2-\Lambda^2)}{J^2(2J-1)(2J+1)} + \frac{[(J+1)^2-M^2][(J+1)^2-\Lambda^2]}{(J+1)^2(2J+1)(2J+3)} + \frac{M^2\Lambda^2}{J^2(J+1)^2} \quad (19c)$$

where  $\Lambda$  and  $M$  are not included explicitly as indices on the  $Q$  terms since they remain unchanged during a transition.

The refractive index can be determined from the induced susceptibility which is obtained from the trace of the product of the operator  $n(\Delta\alpha \cos^2\theta + \alpha_{\parallel})$  and the density matrix obtained from Eq. (17).

The zeroth order of approximation gives the linear refractive index  $n_0$ , which depends only on the values of the density matrix elements prior to the optical disturbance. One readily finds that  $n_0 = \frac{2\pi N}{3} (\alpha_{||} + 2\alpha_{\perp})$  in agreement with the theorem of spectroscopic stability<sup>15</sup> and the previous result from the quadratic Stark shifts.

The lowest order values for the off-diagonal components of the density matrix and the corresponding nonlinear refractive index change can be obtained immediately by replacing the  $Q_{I,J}$  in the results for linear molecules in Ref. 4 by those of Eq. (19). Since the quantum number  $\Lambda$  as well as  $M$  does not change during a rotational transition, the only difference in the final results is an additional sum over the quantum number  $\Lambda$ . Thus the expressions for  $\rho_{J+2,J}$  and  $\Delta n$  (Ref. 4) are rewritten:

$$\rho_{J+2,J} = -i \left[ R_{J+2,J} \int_{t_0}^t \exp(-i\omega_J t') \langle \vec{E} \cdot \vec{E} \rangle dt' \right] \exp(i\omega_J t) \quad (20a)$$

$$\rho_{J,J+2} = \rho_{J+2,J}^* \quad (20b)$$

$$\Delta n(t) = \frac{4\pi N}{n_0} \sum_{J=0}^{\infty} T_J \text{Im} \left[ e^{i\omega_J t} \int_{t_0}^t e^{-i\omega_J t'} \langle \vec{E} \cdot \vec{E} \rangle dt' \right] \quad (21)$$

where  $t_0$  is an initial time for which  $\langle \vec{E} \cdot \vec{E} \rangle$  can be assumed to be zero.  $T_J$  is the double sum

$$T_J = \sum_{M, \Lambda = -J}^J R_{J+2,J} Q_{J+2,J}^{\Delta\alpha} \quad (22)$$

with  $\omega_J = 4\pi Bc(2J+3)$  and  $\text{Im}$ , the imaginary part of the term inside the bracket. As previously,

$$R_{J+2,J} = \left[ \left( \rho_{J,J}^{(0)} - \rho_{J+2,J+2}^{(0)} \right) / 2\hbar \right] Q_{J+2,J} \Delta\alpha \quad (23)$$

where  $\rho_{J,J}^{(0)}$  is the initial zero field thermal equilibrium value of the diagonal component of the density matrix:

$$\rho_{J,J}^{(0)} = \frac{e^{-H_{J,\Lambda}^0/kT}}{\sum_{J=0}^{\infty} \sum_{\Lambda=-J}^J (2J+1) e^{-H_{J,\Lambda}^0/kT}} \quad (24)$$

In the above expression for  $T_J$ , the sum over  $M$  can be explicitly carried out, giving

$$T_J = \frac{(\Delta\alpha)^2}{15\hbar} \sum_{\Lambda=-J}^J \left[ \rho_{J,J}^{(0)} - \rho_{J+2,J+2}^{(0)} \right] \frac{[(J+1)^2 - \Lambda^2][(J+2)^2 - \Lambda^2]}{(J+1)(J+2)(2J+3)} \quad (25)$$

This obviously reduces to the results for a linear molecular gas when  $\Lambda = 0$ .<sup>4</sup>

## V. STATIONARY REFRACTIVE INDEX CHANGE FOR SYMMETRIC TOP MOLECULAR GASES

To evaluate the stationary, intensity-dependent refractive index from Eq. (21), it is assumed that  $\langle \vec{E} \cdot \vec{E} \rangle$  is slowly varying with respect to  $e^{-i\omega_J t}$  and that  $\langle \vec{E} \cdot \vec{E} \rangle$  is zero for  $t' = t_0$ . Integrating Eq. (21) by parts and neglecting time derivatives of  $\langle \vec{E} \cdot \vec{E} \rangle$ , one obtains for any given time  $t$ :

$$\Delta n = \frac{4\pi N}{n_0} \sum_{J=0}^{\infty} \frac{T_J}{\omega_J} \langle \vec{E} \cdot \vec{E} \rangle \quad (26)$$

which is a generalization of Eq. (9) obtained for linear molecules using the time-independent approach.

In the low-temperature limit, Eq. (26) reduces to (15a) since only the level with the lowest energy  $E(J = 0, A = 0, M = 0)$  is populated. In the high-temperature limit, no analytic expression analogous to Eq.(15) can be deduced with assumptions corresponding to those employed for linear molecules. The expression for the induced refractive index change in this case can be conveniently written:

$$\Delta n = F(T) \left[ \frac{2\pi N}{30} \frac{(\Delta\alpha)^2}{kTn_0} \right] \langle \vec{E} \cdot \vec{E} \rangle \quad (27)$$

The coefficient  $F(T)$ , in general, depends on temperature and on the rotational constants  $A$  and  $B$ . Numerical calculations have been made for the  $\text{CH}_3\text{Cl}$  molecule, which has polarizabilities  $\alpha_{||} = 5.42 \times 10^{-24}$  esu and  $\alpha_{\perp} = 4.14 \times 10^{-24}$  esu,<sup>16</sup> and rotational constants  $A = 5.090 \text{ cm}^{-1}$  and  $B = 0.4434 \text{ cm}^{-1}$ .<sup>17</sup> Results show that the coefficient  $F(T)$  for this molecule is 0.8434 at  $T = 296^\circ \text{ K}$  and 0.8461 at  $T = 1000^\circ \text{ K}$ .

For temperatures high enough for  $F(T)$  not to vary significantly ( $\geq 1000^\circ \text{ K}$  for  $\text{CH}_3\text{Cl}$ ), the refractive index change depends on  $A$  and  $B$  only through their ratio. This dependence is indicated in Fig. 5. The coefficient  $F(T)$  decreases with decreasing  $A/B$  to approximately 0.4291 when  $A/B = 1/2$ , which is the value for an "ideal ring molecule." Such a decrease in the value of  $F(T)$  with decreasing  $A/B$  results from the combined effect of the decrease in  $Q_{I,J}$  with increasing  $A$  and the decrease of the unperturbed rotational energy with a decreasing  $A/B$ . The latter implies that the states with high  $A$  (and hence low values of  $Q_{I,J}$ ) are weighted more heavily in the sum over  $A$  in Eq. (26).

The coefficient  $n_2$  and the factor  $F(T)$  of several symmetric top molecular gases are given in Table II.

## VI. COHERENT TIME-DEPENDENT REFRACTIVE INDEX CHANGES IN GASES COMPOSED OF SYMMETRIC TOP MOLECULES

The rotational response of a molecular gas to an optical pulse exhibits a nonnegligible explicit time dependence if the pulse duration is not too long. For symmetric top molecules, such will be the case for durations less than or equal to the inverse of the fundamental quadrupole transition frequency, which is  $1/6Bc$ . The spectral content of the pulse envelope then overlaps the rotational transition frequencies and a significant number of transitions can occur among the Stark shifted rotational states evaluated in § II. These transitions are, of course, not taken into account in the stationary perturbation calculations.

The transitions result in a net absorption of energy by the gas, leaving the rotational population distribution, and hence the refractive index, perturbed after the passage of the pulse.

Such a perturbation can also be interpreted in terms of a transient development, during the optical excitation, of superpositions of pairs of rotational states. At the termination of the excitation, the percentage of each state composing the pair ceases to change, while the relative phase between the two states continues to evolve at a constant rate equal to the transition frequency between the two.

The nonlinear refractive index change subsequent to the optical excitation is described by a collection of such steady-state superposition states, each of which is thus evolving with a well-established phase relationship with respect to the remaining superposition states. The collection is expressed by a Fourier sum that has components at the quadrupole transition

frequencies  $\omega_J = 4\pi Bc(2J+3)$ . Such a sum is obtained from Eq. (21) by extending the upper limit to infinity, this being justified since  $\langle \vec{E} \cdot \vec{E} \rangle$  is zero for all  $t$  subsequent to excitation.

The Fourier component for a particular frequency  $\omega_J$  is the product of the Fourier transform of the optical intensity at frequency  $\omega_J$  and the coefficient  $T_J$  defined by Eq. (25). For linear molecules for which the sum over  $\Lambda$  can be dropped and  $\Lambda$  set to equal to zero, the Fourier sum over the rotational frequency spectrum has been shown to represent short periodic bursts in the refractive index, spaced in time by intervals of  $1/4Bc$ .<sup>4</sup>

A complete analysis of the excited refractive index change, in particular one that includes the response during excitation with the optical pulse and the strength of the subsequent short bursts as a function of pulse width, requires a numerical integration of Eq. (21). Figure 6 illustrates the overall features of the time-dependent refractive index change. This particular example pertains to  $CS_2$  vapor ( $A \rightarrow \infty$ ,  $B = 0.1091 \text{ cm}^{-1}$ )<sup>17</sup> for an optical excitation assumed to have a Gaussian electric field profile given by

$$E = \frac{1}{2} A \exp(-2t^2/\tau^2) (e^{i\omega t} + e^{-i\omega t}) \quad (28)$$

For a relatively long pulse (5 psec or longer), the initial refractive index change closely follows that given by the stationary quartic Stark shift (hence the pulse shape), and the strength of the quantum interference is small compared to that of this initial response. With a reduction in the pulse width (1 psec or shorter), the refractive index change occurring simultaneously with the excitation diminishes. The initial response gradually attains the time profile expected of the burst due to quantum interference. When pulse width  $\tau$  becomes much less than the width of the bursts in refractive index, the entire index change is completely described by the sum over the fully developed or steady-state superposition states.

For symmetric top molecules, the particular Fourier series describing only the refractive index subsequent to excitation by a Gaussian field described by Eq. (28), as determined from Eq. (21), is

$$\Delta n(t) = \pi^{3/2} N \tau A^2 \sum_{J=0}^{\infty} T_J \exp(-\omega_J^2 \tau^2 / 16) \sin \omega_J t \quad (29)$$

The development of the burst in refractive index can be traced by initially considering the evolution of only one of the superposition states represented by this series. For simplicity, a delta function excitation is assumed ( $\exp[-\omega_J^2 \tau^2 / 16] \approx 1, A^2 = 2/\tau$ ) and the  $J = 0$  rotational state is considered at  $t = 0$ . A certain number of the molecules initially in this state will be forced by the optical pulse into a superposition with the  $J = 2$  state, in particular the one for which  $M = 0$ . The wave function of the molecule having undergone such a change can be written as<sup>18</sup>

$$\psi = \frac{i}{\sqrt{2}} \left[ [0] e^{-i\left(\frac{\omega_0 t}{2} - \frac{\pi}{4}\right)} + [2] e^{i\left(\frac{\omega_0 t}{2} - \frac{\pi}{4}\right)} \right] \quad (30)$$

where  $[0]$  stands for the wave function for  $J = 0$  and  $[2]$  stands for the wave function for  $J = 2, M = 0$ . The former is proportional to the zeroth-order and the latter to the second-order ordinary Legendre polynomial. One observes that this superposition of the wave functions gives the proper form for the off-diagonal components of the density matrix elements in Eq. (20) and the



phase evolves at a rate  $\omega_0$  as stated earlier. The probability density functions  $|\psi(t)|^2$  for times  $t = 0, \pi/2\omega_0, \pi/\omega_0$ , and  $3\pi/2\omega_0$ , subsequent to excitation and the differences  $|\psi(t)|^2 - |\psi(0)|^2$ , which are proportional to the induced anisotropy, are shown in Fig. 7.

At  $t = 0$ , immediately after the perturbation is applied, the two states are superposed in quadrature. This leads to the most uniform angular distribution of the total probability amplitude and implies that the molecules remain in a random orientation just after the perturbation. However, the state evolves so that, at a time equal to  $1/4$  the transition period, the probability amplitude is highly peaked in the direction of the electric field, i.e., the molecules tend to be oriented along the direction of the field. After another fourth of a period, the probability amplitude is distributed uniformly once more. Three-fourths of a period after the disturbance, the probability function is peaked again, but in a direction perpendicular to the applied field. We see from Figs. (7e) and (7f) that the net anisotropy of the probability density function at  $\omega_0 t = 3\pi/2$  is equivalent to that at  $\omega_0 t = \pi/2$ , but in the perpendicular direction. The wave function returns to the original superposed state at the end of a full period. This behavior occurs periodically as expressed by this sinusoidal evolution of the superposition state.

In general, the state with angular momentum quantum numbers  $J, M$  will be superimposed with a state with quantum numbers  $J+2, M$  or  $J-2, M$  and any of these superposed states behaves in a manner completely analogous to the one discussed above. In particular, the evolution of the superposed state consisting of a

linear combination of the eigenstates of  $J$  and  $J+2$  can be represented by the phase factor  $\exp(i\omega_J t)$  in Eq. (21).

In general, the width and shape of the bursts in the refractive index change depend on the width of the excitation pulse as well as the spectral content of the coefficients  $T_J$ . When the pulse is very short so that the Fourier spectrum is essentially constant over the dominating rotational transition frequencies, the spectral content of the refractive index is limited by the spectral width of  $T_J$ . The relative amplitude of  $T_J$  as a function of  $J$  is plotted in Fig. 8 for  $\text{CS}_2$  vapor at  $296^\circ\text{K}$ . The effective rotational levels range roughly from  $J = 20$  to  $70$ , which gives a bandwidth of  $\Delta f = 4Bc(70-20) = 6.5 \times 10^{11} \text{ sec}^{-1}$ . Hence the width of the complete burst, covering both the positive peak and the negative peak, is approximately  $\Delta \tau = 1/\Delta f = 1.5 \times 10^{-12} \text{ sec}$ . The full width of either peak at half the maximum amplitude is about  $1/3$  of this value or  $0.5 \times 10^{-12} \text{ sec}$ .

For the opposite extreme, that of a pulse having a spectral width for which only relatively few of the thermally populated energy levels are excited, the width of the burst is roughly proportional to the pulse width.

Both extremes in excitation pulse width, extremely short or extremely long, produce a small number of superposed states and consequently quantum interference strength. The most efficient utilization of a burst of optical energy occurs when it is contained in a time duration that is roughly the inverse of the frequency of the dominating rotational transitions. Since for large  $J$ , for linear molecules,  $T_J$  is approximately proportional to  $J^2 \exp(-J^2 hBc/kT)$ , the level with the maximum value for this factor is given by  $J_{\max} = (kT/hBc)^{1/2}$ , which for  $\text{CS}_2$  at  $296^\circ\text{K}$  is approximately  $44$ .<sup>4</sup> The optimum pulse width is the inverse of  $4Bc J_{\max}$

$$\tau_{\text{op}} \approx \frac{1}{4Bc} \left[ \frac{hBc}{kT} \right]^{1/2} = 5 \times 10^{-12} (BT)^{-1/2} \quad (31)$$

A numerical calculation over a temperature range  $100^\circ$  to  $1200^\circ\text{K}$  for different values of  $B$  gives  $\tau_{\text{op}} = 4.5 \times 10^{-12} (BT)^{-1/2}$  in close agreement with this approximation expression. Figure 9, in which the peak amplitude of the refractive index in  $\text{CS}_2$   $1/4 Bc$  after excitation is plotted as a function of excitation pulse duration, illustrates the range about the optimum pulse width which can be tolerated without decreasing the strength of the echo significantly.

Computed refractive index profiles due to quantum interference induced by Gaussian-shaped light beams in  $\text{CS}_2$  vapors and  $\text{CH}_3\text{Cl}$  vapors at  $296^\circ\text{K}$  are plotted in Fig. 10 for various pulse widths. One notes that the normalization constant for the latter is  $\Delta n_s = F(T)[2\pi N(\Delta\alpha)^2/30kTn_0]$ , with  $F(T) = 0.8434$ .

Comparing Fig. (10a) with (10b), we see that the time profiles are almost the same for the linear and symmetric top molecules. They are both antisymmetric since the fundamental frequency of the Fourier components in both cases is  $2B$  and the function is odd. On the other hand, for the symmetric top, the normalized refractive index change can be larger than unity in contrast to that of the linear molecule. For  $\text{CH}_3\text{Cl}$  vapor, it is 1.08 at room temperature. However, since  $\Delta n_s = 0.843 \Delta n_m$ , the amplitude is still smaller than that of a linear molecule having the same rotational constant  $B$  and the same polarizability anisotropy  $\Delta\alpha$ . In addition, for the symmetric top molecule, the level of maximum contribution tends to have

a high  $J$  value and hence an optimum pulse width shorter than that of the linear molecule. Consequently, the width of the burst is also shorter for the symmetric top molecule. (This width cannot be computed from Eq. (31).)

Table III lists the optimum pulse widths and echo periods for several gases at 296°K. The widths have been obtained from Eq. (31) for linear molecules and numerically for the remaining ones.  $\text{CS}_2$  and benzene appear particularly favorable for initial investigations. They both have large anisotropies and relatively small rotational constants and require optimum pulse widths that could be achieved with present mode-locked lasers.

Interference with the rotational coherence will arise from collisional and Doppler effects. Significantly populated excited vibrational levels as well as the centrifugal stretching parameter could also interfere with the rotational coherence, provided the rotational constants vary significantly.

For  $\text{CS}_2$ , the rotational constant is hardly effected by centrifugal stretching (for the level with  $J = 200$ , the increase in rotational constant is 0.01%). In addition, the rotational constant of the vibrationally excited molecules is barely different from that of the unexcited ones. Hence, though 11% of the molecules are in the first excited state, the induced refractive index should not be changed appreciably. Note that the lowest vibrational levels of benzene is above the highly populated rotational levels. In addition, the small centrifugal stretching parameters coupled with a small rotational constant and a large anisotropy in polarizability make this particularly favorable as well.<sup>24</sup>

# VII. INTEGRATED STRENGTH AND DETECTION OF THE REFRACTIVE INDEX RESPONSE

Although the amplitude of the refractive index change subsequent to optical excitation is highly dependent on the optical pulse duration, the time integration of the entire induced refractive index response depends only on the energy of the exciting pulse and not on its duration.

From expression (21), the total area  $A_T$  is given by

$$A_T = \frac{4\pi N}{n_o} \sum_{J=0}^{\infty} T_J \text{Im} \left[ \int_{-\infty}^{\infty} e^{i\omega_J t} \int_{-\infty}^t \langle \vec{E} \cdot \vec{E} \rangle e^{-i\omega_J t'} dt' dt \right] \quad (32)$$

For generality,  $\langle \vec{E} \cdot \vec{E} \rangle$  is assumed to have an arbitrary time profile, although Gaussian-shaped pulse envelopes are reasonably justified for most Q-switched and perhaps mode-locked laser pulses. Rather than obtaining a delayed refractive index burst that is antisymmetric about its center of gravity, Eq. (21) shows that the asymmetric part of the optical pulse gives rise to a superposed contribution that is symmetric about the center of gravity. For example, Fig. 11 illustrates a sequence of bursts induced in  $\text{CS}_2$  gas at room temperature by an optical excitation with both symmetric and antisymmetric components of the intensity as specified by

$$\langle \vec{E} \cdot \vec{E} \rangle = A_o(t) + A_e(t) \quad (33a)$$

where

$$A_o(t) = \left\{ C_1 \exp[-4(t+\tau/4)^2/\tau^2] - \exp[-4(t-\tau/4)^2/\tau^2] \right\} \quad (33b)$$

$$A_e(t) = C_2 \exp[-4t^2/\tau^2] \quad (33c)$$

and  $C_1$  and  $C_2$  are constants.

It is evident that the net contribution to the total time integrated refractive index change is zero subsequent to  $t = (8Bc)^{-1}$  for the portion of the excitation which is an even function of  $t$  and subsequent to  $t = (4Bc)^{-1}$  for that which is an odd function of  $t$ . Thus we need consider only times less than these for the two contributions, respectively. Changing the order of integration for each of these in Eq. (32) and explicitly carrying out the integration with respect to  $t$ ; one obtains

$$A_T = \frac{4\pi N}{n_o} \sum_{J=0}^{\infty} \frac{T_J}{\omega_J} \left[ \int_{-\infty}^{\frac{1}{8Bc}} A_e(t') dt' + \int_{-\infty}^{\frac{1}{4Bc}} A_o(t') dt' \right] \\ - \frac{4\pi N}{n_o} \sum_{J=0}^{\infty} \frac{T_J}{\omega_J} \left[ \int_{-\infty}^{\frac{1}{8Bc}} A_e(t') \sin \omega_J t' dt' + \int_{-\infty}^{\frac{1}{4Bc}} A_o(t') \cos \omega_J t' dt' \right] \quad (34)$$

If the pulse width  $\tau$  is shorter than  $(8Bc)^{-1}$ , where  $\tau$  is the full width at half intensity, the upper limit of the integration can be extended to infinity.

From symmetry, the second set of bracketed terms vanishes after the integration.

The total area reduces to

$$A_T = \frac{4\pi N}{n_o} \sum_{J=0}^{\infty} \frac{T_J}{\omega_J} \int_{-\infty}^{\infty} \langle \vec{E} \cdot \vec{E} \rangle dt \quad (35)$$

which is just the total area that would be obtained from a stationary calculation.

The upper integration limits can be taken without loss of generality as  $1/8Bc + n/2Bc$  and  $1/4Bc + n/2Bc$ , respectively, for even and odd components of the excitation, where  $n$  is a positive integer. Thus, Eq. (34) is applicable for pulses of duration  $(8Bc)^{-1}$  or larger. However, for pulses having such a long duration, the strength of the quantum interference is negligible and the refractive index is given very well by the stationary result.

The experimental detection of the transient portion of the refractive index change should, according to the above, roughly depend only on the total energy of the optically exciting pulse. This is true for a detection technique that produces a signal linearly proportional to the birefringence<sup>2</sup> and a probe pulse of the same duration as the birefringence pulse. The recent technique for probing short-duration birefringence employed by Duguay and Hansen<sup>19</sup> involves the square of the birefringence for which the detected signal will increase with a decrease in the exciting pulse width up to the point at which the birefringence becomes independent of the pulse width.

The detectability of the delayed bursts in refractive index for several molecular species is tabulated in Table IV. As for Table III, the optimum length of the excitation pulse has been estimated numerically for symmetric top molecules and from Eq. (31) for linear molecules. The maximum relative phase shift between the electric field components perpendicular to and parallel to the polarization direction of the excitation pulse and produced by the refractive index burst has also been listed as  $\Delta\phi$ . This has been evaluated for a length of 1 m, at a wavelength of  $0.53\mu$ , and for a peak power density of  $500 \text{ MW/cm}^2$  for the excitation. The resultant fraction of energy which would be transmitted through an analyzing polarizer has been estimated assuming the probe pulse to be centered on the peak of the refractive index profile for the 1 m length and, in addition, that it is much shorter than the

duration of the refractive index profile. Consequently, this is the optimum value that would be obtained. If the probe pulse is of the order of the width of the echoic response then one would expect this to be reduced by approximately a factor of 2.

The resultant signal-to-noise ratios that can be achieved for the rather conservative optical intensity chosen are encouraging. This has been obtained as the ratio of the above percentage of the energy of the probe pulse which is transmitted by the crossed polarizers due to the echoic response to that which would be transmitted in the absence of the echoic response. The latter is primarily determined by the extinction ratio of the polarizer pair, which can be of the order of  $10^{-6}$ . Scattering due to the vapor and the window of the sample cell have not been included but should not present any difficulty.

#### VIII. CONCLUSIONS

The sequence of refractive index bursts, which is essentially the rotational response of the molecule to a delta function excitation, should be useful for various spectroscopic measurements. The spacing between the bursts provides a direct measurement of the rotational constant of symmetric top molecules. This method would be particularly convenient for relatively large organic molecules that possess a center of inversion, such as pyrene. For conventional spectroscopic approaches, broadening would cause the rotational transitions to merge. In the time domain, however, the bursts are diminished in amplitude due to Doppler or collisional effects but should still be detectable. This result together with the fact that molecules with large moments of inertia exhibit a relatively long ( $\approx 3 \times 10^{-9}$  sec for pyrene) delay before the appearance of the refractive index change and an optimum pulse width that



is longer ( $\approx 2 \times 10^{-12}$  sec for pyrene at  $296^{\circ}\text{K}$ ) provide an advantage.

The transient response in the refractive index should also provide a useful means of studying collisional phenomena in gases. Even the factor of  $3/4$  reduction of the collisionless stationary value of  $n_2$  with respect to the thermodynamic equilibrium value should be significant enough to be easily detected.

# APPENDIX A: LINEAR MOLECULAR STARK SHIFTS

The eigenvalues associated with the spheroidal wave functions have been given in a power series expansion.<sup>5</sup> To evaluate the refractive index, it is convenient to rewrite the coefficient for each power of the perturbation parameter in terms of a common denominator and to arrange the numerator in a descending series in terms of powers of quantum number M. The first three terms are given in § III;  $\lambda_3$  and  $\lambda_4$  are, respectively,

$$\lambda_3 = \frac{Q_6 M^6 + Q_4 M^4 + Q_2 M^2 + Q_0}{(2J-5)(2J-3)(2J-1)^5(2J+1)(2J+3)^5(2J+5)(2J+7)} \quad (A1a)$$

$$\lambda_4 = \frac{R_8 M^8 + R_6 M^6 + R_4 M^4 + R_2 M^2 + R_0}{16(2J-7)(2J-5)^2(2J-3)^3(2J-1)^7(2J+1)(2J+3)^7(2J+5)^3(2J+7)^2(2J+9)} \quad (A1b)$$

where

$$\begin{aligned} Q_0 &= -4(140J^9 + 720J^8 + 688J^7 - 952J^6 - 1758J^5 \\ &\quad - 335J^4 + 798J^3 + 576J^2 + 91J - 15) \\ Q_2 &= 8(320J^9 + 1440J^8 + 1600J^7 - 1120J^6 - 2172J^5 \\ &\quad + 730J^4 + 2106J^3 + 909J^2 + 735J + 315) \\ Q_4 &= -4(1792J^7 + 6272J^6 + 11040J^5 + 11920J^4 \\ &\quad + 6656J^3 + 1200J^2 + 6834J + 3465) \\ Q_6 &= 16(288J^5 + 720J^4 + 2576J^3 + 3144J^2 + 2410J \\ &\quad + 705) \end{aligned}$$

$$\begin{aligned}
R_0 = & 2621440J^{22} + 28835840J^{21} + 67502080J^{20} - 334233600J^{19} \\
& - 1652391936J^{18} + 406880256J^{17} + 12640935936J^{16} \\
& + 11465981952J^{15} - 47151794176J^{14} - 86929668096J^{13} \\
& + 60776768000J^{12} + 283966432256J^{11} + 179093012352J^{10} \\
& - 331641182336J^9 - 597523865568J^8 - 39584051328J^7 \\
& + 562799872768J^6 + 305661829696J^5 - 144966710848J^4 \\
& - 144459953280J^3 - 23823704448J^2 + 1681374240J \\
& - 123832800
\end{aligned}$$

$$\begin{aligned}
R_2 = & - 132120576J^{20} - 1321205760J^{19} - 2986868736J^{18} \\
& + 10772545536J^{17} + 55153655808J^{16} + 26351763456J^{15} \\
& - 230151454720J^{14} - 364095176704J^{13} + 213326028800J^{12} \\
& + 709242830848J^{11} - 39055316992J^{10} - 538931681280J^9 \\
& + 423846592000J^8 + 536931813376J^7 - 796268822912J^6 \\
& - 1151804954752J^5 - 44866063232J^4 + 732693962880J^3 \\
& + 534689631360J^2 + 153715363200J + 15812496000
\end{aligned}$$

$$\begin{aligned}
R_4 = & 858783744J^{18} + 7729053696J^{17} + 16658989056J^{16} \\
& - 41919971328J^{15} - 235709202432J^{14} - 303193325568J^{13} \\
& + 358526828544J^{12} + 1907821019136J^{11} \\
& + 2395260653568J^{10} - 1479590572032J^9 \\
& - 5776834200576J^8 - 1235455438848J^7 + 5280868948224J^6 \\
& + 1601948246784J^5 - 3438094991424J^4 - 1925582232960J^3 \\
& - 1295953634304J^2 - 1226174604480J - 338863694400
\end{aligned}$$

$$\begin{aligned}
R_6 = & - 1499463680J^{16} - 11995709440J^{15} - 28251258880J^{14} \\
& + 12166103040J^{13} + 263258767360J^{12} + 875588485120J^{11} \\
& + 691770327040J^{10} - 2847928647680J^9 \\
& - 6429128499200J^8 - 2067620659200J^7 \\
& + 5728792217600J^6 + 6081225021440J^5 + 2478926763520J^4 \\
& + 1276743582720J^3 + 4306275239040J^2 + 3691965916800J \\
& + 877688784000
\end{aligned}$$

$$\begin{aligned}
R_8 = & 770179072J^{14} + 5391253504J^{13} + 15384051712J^{12} \\
& + 22218014720J^{11} - 103817510912J^{10} - 594261147648J^9 \\
& - 647287250944J^8 + 1000544829440J^7 \\
& + 3448504383488J^6 + 4334596040704J^5 \\
& - 611972320768J^4 - 6087058191360J^3 \\
& - 6531288018048J^2 - 3111137285760J - 554513752800
\end{aligned}$$

The last three terms, which give rise to the nonlinear refractive index change, were discussed in the text. The second term gives the total quadratic Stark shift for each J level. The expectation value is

$$\langle \Delta W_1 \rangle = hBcK \frac{\sum_{J=0}^{\infty} -\frac{1}{3} (2J+1) e^{-J(J+1)\eta}}{\sum_{J=0}^{\infty} (2J+1) e^{-J(J+1)\eta}} = -\frac{1}{6} \Delta \alpha E^2. \quad (A2)$$

Thus each J level contributes equally to the linear refractive index,

$$1 + \frac{2}{3} \pi N (\alpha_{||} + 2\alpha_{\perp}).$$

APPENDIX B: OPTICALLY-INDUCED REFRACTIVE INDEX FOR  
THERMAL EQUILIBRIUM

The intensity-dependent portion of the nonlinear refractive index change arising from the Stark shifts of the rotational levels, which are assumed to be in thermo-dynamic equilibrium at temperature  $T$ , can be deduced from an average of the perturbed energy. We wish to obtain the high-temperature limit and show that it is equivalent to that given by the classical calculation.

The partition function including the quartic Stark terms is given by

$$\sigma = \sum_{J=0}^{\infty} \sum_{M=-J}^{+J} e^{-E_J/kT} e^{1/kT(\partial_{J,M}P + \beta_{J,M}P^2)} \quad (B1)$$

where

$$E_J = hBcJ(J+1)$$

$$P = \frac{\Delta\alpha}{2} E^2$$

$$\partial_{J,M} = \lambda_1(J,M)$$

$$\beta_{J,M} = -\frac{\lambda_2(J,M)}{hBc}$$

The terms  $\lambda_1(J,M)$  and  $\lambda_2(J,M)$  are given in § III.

Following the procedure used by Debye,<sup>1</sup>  $\sigma$  is expanded in powers of  $P$ .<sup>23</sup>

Defining the summations

$$\left. \begin{aligned} \sigma_0 &= \sum_{J,M} e^{-\frac{E_J}{kT}} \\ \sigma_2 &= \sum_{J,M} \partial_{J,M} e^{-\frac{E_J}{kT}} \end{aligned} \right\} \quad (B2)$$

$$\left. \begin{aligned} \sigma'_2 &= \sum_{J,M} 2\beta_{J,M} e^{-\frac{E_J}{kT}} \\ \sigma''_2 &= \sum_{J,M} \beta_{J,M}^2 e^{-\frac{E_J}{kT}} \end{aligned} \right\} \quad (\text{B2 Cont})$$

and

$$\sigma_2 = \sigma'_2 + \frac{1}{kT} \sigma''_2$$

the result to terms in  $P^2(E^4)$  terms is

$$\sigma = \sigma_0 + \frac{\sigma_1}{kT} P + \frac{\sigma_2}{2kT} P^2 \quad . \quad (\text{B3})$$

Retaining only the significant components up to the second order in  $P$ , the Helmholtz free energy is

$$\begin{aligned} \phi &= -kT \log \sigma \\ &= -kT \log \sigma_0 - P \left( \frac{\sigma_1}{\sigma_0} \right) - \frac{P^2}{2} \left[ \frac{\sigma_2}{\sigma_0} - \frac{1}{kT} \left( \frac{\sigma_1}{\sigma_0} \right)^2 \right] \end{aligned} \quad (\text{B4})$$

where

$$\frac{\sigma_1}{\sigma_0} = \frac{1}{3} \quad , \quad \left( \frac{\sigma_1}{\sigma_0} \right)^2 = \frac{1}{9}$$

and in the high-temperature limit,

$$\frac{\sigma'_2}{\sigma_0} = \frac{2}{30} \frac{1}{kT}$$

$$\frac{\sigma''_2}{\sigma_0} = \frac{2}{15} + \left( \frac{1}{15} \right) \frac{\sum_{J=0}^{\infty} \frac{2J+1}{(2J-1)(2J+3)} e^{-E_J/kT}}{\sum_{J=0}^{\infty} (2J+1) e^{-E_J/kT}} \quad . \quad (\text{B5})$$

The last term in Eq. (B5) is a function of temperature and approaches zero as T goes to infinity. A numerical calculation shows that at  $hBc/kT = 5 \times 10^{-4}$  ( $CS_2$  at room temperature) the entire term is approximately  $10^{-5}$ . The first term in Eq. (B4) corresponds to the unperturbed potential energy of the molecules. The second term

$$\langle \Delta W_1 \rangle = - \frac{1}{3} \left( \frac{\Delta \alpha}{2} E^2 \right) \quad (B6)$$

contributes to the electric-field independent dielectric constant. The last set of terms gives

$$\langle \Delta W_2 \rangle = - \frac{2}{45} \frac{1}{kT} \left( \frac{\Delta \alpha}{2} E^2 \right)^2 \quad (B7)$$

which implies that the nonlinear index of refraction coefficient  $n_2$  is

$$n_2 = 2\pi N \left( \frac{2}{45} \right) \left( \frac{(\Delta \alpha)^2}{kT n_o} \right) \quad (B8)$$

where N is the number of molecules per unit volume. This is exactly the classic result.<sup>3</sup>

It is interesting to observe that whereas the classical partition function contains only the term  $\frac{1}{2} (\Delta \alpha) E^2$ ; the quartic Stark shift, an energy term propotional to  $E^4$  is necessary to evaluate  $n_2$  quantum mechanically.

APPENDIX C: QUARTIC STARK SHIFT CALCULATED FROM THE  
TIME-DEPENDENT PERTURBATION OF THE DENSITY MATRIX

It is instructive to evaluate the stationary value of the quartic Stark shift from the internal energy (expectation of the Hamiltonian). This necessitates, in addition to the first order perturbed values of the off-diagonal components of the density matrix, the perturbed values of the diagonal components. Working from the density matrix equations, it is sufficient to assume that the electric-field intensity is applied slowly with respect to the inverse of the rotational transition frequencies of the molecules. In this manner, the terms involving transitions among the Stark shifted levels do not enter. Thus, we consider a perturbing Hamiltonian with the following conditions:

$$H' = -\frac{1}{2} \Delta \alpha E_0^2 T(t) \cos^2 \theta \quad (C1)$$

$$T(t) = 0, \quad t \leq 0$$

$$\frac{dT(t)}{dt} \geq 0, \quad \frac{d^m T(t)}{dt^m} \ll (\omega_J)^m T(t), \quad t > 0$$

where  $m$  is any positive integer. Substituting this perturbation function in Eq. (C1) and using successive partial integration, the integral in the equation can be expanded in a series involving the above time derivatives.

Thus

$$\int_0^t H'_{J,J-2}^M e^{i\omega_{J-2}t'} dt' = D_{J,J-2}^M \left[ \frac{T(t') e^{i\omega_{J-2}t'}}{i\omega_{J-2}} + \frac{\frac{dT(t')}{dt'} e^{i\omega_{J-2}t'}}{\omega_{J-2}^2} + \frac{\frac{d^2T(t')}{dt'^2} e^{i\omega_{J-2}t'}}{i\omega_{J-2}^3} + \dots \right]_0^t \quad (C2)$$



Where  $Q_{J,J-2}^M$  is defined in Eq. (15) and  $D_{J,J-2}^M = \Delta\alpha\langle E_0^2 \rangle / 2 \times Q_{J,J-2}^M$ . Because of the last condition in Eq. (C2), this expression can be approximated by the first two terms, and the off-diagonal elements become

$$\rho_{J,J-2}^{(1)} = D_{J,J-2}^M \left[ \rho_{J,J}^{(0)} - \rho_{J-2,J-2}^{(0)} \right] \left[ \frac{T(t)}{\hbar\omega_{J-2}} + \frac{i \frac{dT(t)}{dt}}{\hbar\omega_{J-2}^2} \right] \quad (C3)$$

The perturbation of the diagonal elements, obtained by substituting  $\rho_{J,I}^{(1)}$  for the off-diagonal elements into Eq. (13) and integrating, is

$$\begin{aligned} \rho_{J,J}^{(2)} &= (D_{J,J-2}^M)^2 \left[ \rho_{J,J}^{(0)} - \rho_{J-2,J-2}^{(0)} \right] \int_0^t \frac{-\frac{dT(t')}{dt'} T(t')}{\hbar^2 \omega_{J-2}^2} dt' \\ &= \left[ \rho_{J-2,J-2}^{(0)} - \rho_{J,J}^{(0)} \right] \left[ \frac{D_{J,J-2}^M T(t)}{\hbar\omega_{J-2}} \right]^2 \end{aligned} \quad (C4)$$

The expectation of the quartic Stark shift, given by the trace of the product of the density matrix and the Hamiltonian, is given by

$$\langle \Delta W_2 \rangle = [T(t)]^2 \sum_{J=0}^{\infty} \sum_{M=-J}^J \left[ \frac{|D_{J,J-2}^M|^2}{\hbar\omega_{J-2}} - \frac{|D_{J,J+2}^M|^2}{\hbar\omega_J} \right] \rho_{J,J}^{(0)} \quad (C5)$$

It can be easily shown that, inside the bracket, the term with any particular quantum number  $J, M$  is exactly  $\hbar B K^2 \lambda_2$ , the quartic Stark shift given in § III.

## FOOTNOTES

\*NRC Postdoctoral Fellow from December 1971 to January 1973. Present address:  
Laboratory for Laser Energetics, University of Rochester, Rochester, New  
York 14627

Work supported by Joint Services Electronics Program Contract USAF-F44620-  
71-C-0087 and NASA Grant NGR-05-003-559.

<sup>5</sup>Contribution No. 3018 from the Department of Chemistry; work partially sup-  
ported by a grant from the National Science Foundation; Alfred P. Sloan  
Fellow.

<sup>1</sup>P. Debye, Polar Molecules (Dover, New York, 1945).

<sup>2</sup>A. D. Buckingham and R. L. Disch, Proc. Roy. Soc. 237A, 275 (1963).

<sup>3</sup>N. Bloembergen and P. Lallemand, Phys. Rev. Letters 16, 81 (1966).

<sup>4</sup>C. H. Lin, J. P. Heritage, and T. K. Gustafson, Appl. Phys. Letters 19,  
397 (1971).

<sup>5</sup>M. Abramowitz and I. A. Segan, Eds., Handbook of Mathematical Functions  
(Dover, New York, 1965), p.754.

<sup>6</sup>C. H. Townes and A. L. Schawlow, Microwave Spectroscopy (McGraw-Hill, New  
York, 1966).

<sup>7</sup>M. E. Mack, R. L. Carman, J. Reintjes, and N. Bloembergen, Appl. Phys.  
Letters 16, 209 (1970).

<sup>8</sup>T. E. Stern, Proc. Roy. Soc. (London) A130, 551 (1931).

<sup>9</sup>R. F. Curl, Jr., H. P. Hopkins, Jr., and K. S. Pitzer, J. Chem. Phys. 48,  
4064 (1968).

<sup>10</sup>L. Pauling, Phys. Rev. 36, 430 (1930).

- <sup>11</sup>G. Herzberg, Spectra of Diatomic Molecules (Van Nostrand Reinhold, New York, 1950).
- <sup>12</sup>The analysis of this section, which has been confined to linearly polarized optical fields, can be easily adapted to circularly polarized fields. The  $i$ th order coefficient of the refractive index change induced by the latter denoted by  $n_i^c$ , is related to  $n_i$  by the simple relationship:  

$$n_i^c = \left(-\frac{1}{2}\right)^{i/2 + 1} n_i$$
- <sup>13</sup>L. D. Landau and E.M. Lifshitz, Statistical Physics (Addison-Wesley, Reading, Mass. 1969).
- <sup>14</sup>P. C. Cross and R. M. Hainer, J. Chem Phys. 12, 210 (1944).
- <sup>15</sup>J. H. Van Vleck, Theory of Electric and Magnetic Susceptability (Oxford Univ. Press, London, 1932).
- <sup>16</sup>J. O. Hershfelder, C. F. Curties, and R. B. Bird, Molecular Theory of Gases and Liquids (Wiley and Sons, Inc., New York, 1954).
- <sup>17</sup>G. Herzberg, Electronic Spectra and Electronic Structure of Polyatomic Molecules (Van Nostrand Reinhold, New York, 1966).
- <sup>18</sup>R. H. Dicke, Phys. Rev. 93, 99 (1954).
- <sup>19</sup>M. A. Duguay and J. W. Hansen, Appl. Phys. Letters 15, 192 (1969).
- <sup>20</sup>Vinod Prakash Krishnaji, Rev. Mod. Phys. 38, 690 (1966).
- <sup>21</sup>R. H. Dicke, in Quantum Electronics, Edited by Grivet and N. Bloembergen (Columbia Univ. Press, New York, 1963), p. 35.
- <sup>22</sup>N. Bloembergen has pointed out that a superradiant state is "... one in which an expectation value of the off diagonal element of the density matrix exists" (see Ref. 20, p. 54).
- <sup>23</sup>There is an error in Eq.(111) of Ref. 1. A factor of  $kT$  should multiply the last term on the righthand side. The equations following should change accordingly.

<sup>24</sup>The observation of the optically induced retractive index and the first delayed burst in refractive index in CS<sub>2</sub> vapor has recently been reported. J. P. Heritage, C. H. Lin, and T. K. Gustafson, Digest of Technical Papers, VIII International Quantum Electronics Conference, p. 48, June, 1974.

<sup>25</sup>"Echo-like" where "echo" according to the American College Dictionary is in classical mythology "A mountain nymph who pined away for love of the beautiful youth Narcissus until only her voice remained".

TABLE I. Nonlinear coefficient  $n_2$  for collisionless gases composed of linear molecules.

|                               | Temperature,<br>(°K) | $\Delta\alpha \cdot 10^{25}$ ,<br>esu | B,<br>cm <sup>-1</sup> | $n_2 \cdot 10^{12}$ ,<br>esu/mole |
|-------------------------------|----------------------|---------------------------------------|------------------------|-----------------------------------|
| CS <sub>2</sub>               | 300                  | 75.0 <sup>a</sup>                     | 0.1092 <sup>d</sup>    | 171.0                             |
| CO <sub>2</sub>               | 300                  | 20.3 <sup>b</sup>                     | 0.3902 <sup>d</sup>    | 12.6                              |
| C <sub>2</sub> H <sub>2</sub> | 300                  | 27.9 <sup>b</sup>                     | 1.177 <sup>d</sup>     | 23.7                              |
| N <sub>2</sub> O              | 300                  | 27.9 <sup>b</sup>                     | 0.4116 <sup>d</sup>    | 23.7                              |
| N <sub>2</sub>                | 300                  | 9.3 <sup>b</sup>                      | 2.001 <sup>e</sup>     | 2.56                              |
| O <sub>2</sub>                | 300                  | 11.4 <sup>b</sup>                     | 1.438 <sup>e</sup>     | 3.94                              |
| HCl                           | 300                  | 7.4 <sup>b</sup>                      | 10.44 <sup>e</sup>     | 1.53                              |
| HBr                           | 300                  | 9.1 <sup>b</sup>                      | 8.360 <sup>e</sup>     | 2.35                              |
| H <sub>2</sub>                | 35                   | 3.02 <sup>c</sup>                     | 59.30 <sup>e</sup>     | 0.434                             |
| D <sub>2</sub>                | 39                   | 2.92 <sup>c</sup>                     | 29.90 <sup>e</sup>     | 0.803                             |

<sup>a</sup>R. Y. Chiao, E. Garmire, and C. H. Townes, Phys. Rev. Letters 13, 479 (1964).

<sup>b</sup>Ref. 16.

<sup>c</sup>K. B. MacAdam and N. F. Ramsey, Phys. Rev. A6, 898 (1972).

<sup>d</sup>Ref. 17.

<sup>e</sup>Ref. 11.

TABLE II. Nonlinear coefficient  $n_2$  for collisionless gases composed of symmetric top molecules at 296°K.

|                               | A, <sup>a</sup><br>cm <sup>-1</sup> | B, <sup>a</sup><br>cm <sup>-1</sup> | $\Delta\alpha \cdot 10^{25},$ <sup>b</sup><br>esu | F(T)  | $n_2 \cdot 10^{12},$<br>esu/mole |
|-------------------------------|-------------------------------------|-------------------------------------|---------------------------------------------------|-------|----------------------------------|
| CH <sub>3</sub> Cl            | 5.090                               | 0.4434                              | 12.8                                              | 0.843 | 4.27                             |
| C <sub>2</sub> H <sub>6</sub> | 2.538                               | 0.6621                              | 15.1                                              | 0.722 | 5.09                             |
| C <sub>6</sub> H <sub>6</sub> | 0.0948                              | 0.1896                              | -59.6                                             | 0.429 | 47.0                             |
| NH <sub>3</sub>               | 6.196                               | 9.444                               | 2.40                                              | 0.436 | 0.0776                           |

<sup>a</sup>See Ref. 17.

<sup>b</sup>See Ref. 16.

TABLE III. Time separation between refractive index bursts and the optimum width of the optical excitation at 296°K.

|                               | $\tau_d = 1/4Bc$<br>$\times 10^{12}$ sec | $\tau_{op}$<br>$\times 10^{12}$ sec |
|-------------------------------|------------------------------------------|-------------------------------------|
| CS <sub>2</sub>               | 76.32                                    | 0.80                                |
| CO <sub>2</sub>               | 21.37                                    | 0.42                                |
| N <sub>2</sub> O              | 20.26                                    | 0.41                                |
| CH <sub>3</sub> Cl            | 17.02                                    | 0.35                                |
| C <sub>2</sub> H <sub>6</sub> | 12.59                                    | 0.29                                |
| C <sub>6</sub> H <sub>6</sub> | 43.98                                    | 0.47                                |

TABLE IV. Detectability of refractive index bursts for gases at 1 atm pressure for a propagation length of 1 m. The peak electric field intensity of the inducing optical pulse is assumed to be  $2 \times 10^3$  esu, and the wavelength of the probe beam is 0.53  $\mu\text{m}$ .  $E_{\parallel}$  is the electric-field component of the probe pulse which is parallel to the electric field of the excitation pulse;  $E_{\perp}$  is that perpendicular to the excitation pulse field.

| Substance                     | Temperature<br>°K | Optimum                       | $n_2(T,P),$<br>esu/cm <sup>3</sup> | Relative phase                                                    | Fraction of<br>diode pulse energy<br>transmitted, $(\Delta\phi/2)^2$ |
|-------------------------------|-------------------|-------------------------------|------------------------------------|-------------------------------------------------------------------|----------------------------------------------------------------------|
|                               |                   | pulse width<br>$10^{-12}$ sec |                                    | shift of $E_{\parallel}$ and $E_{\perp}$<br>$\Delta\phi$ , radian |                                                                      |
| CS <sub>2</sub>               | 319               | 0.77                          | $7.2 \times 10^{-15}$              | 0.26                                                              | 0.017                                                                |
| N <sub>2</sub> O              | 296               | 0.41                          | $1.07 \times 10^{-15}$             | 0.038                                                             | $3.6 \times 10^{-4}$                                                 |
| C <sub>6</sub> H <sub>6</sub> | 353               | 0.43                          | $1.60 \times 10^{-15}$             | 0.057                                                             | $8.1 \times 10^{-4}$                                                 |
| CH <sub>3</sub> Cl            | 296               | 0.37                          | $1.91 \times 10^{-16}$             | 0.0068                                                            | $1.2 \times 10^{-15}$                                                |

# FIGURE CAPTIONS

Figure 1. The lowest Stark shifted rotational energy levels for a fixed electric-field intensity. Those arising from a permanent dipole moment are illustrated on the left-hand side and those arising from the induced dipole moment are shown on the right-hand side. The Stark shifts of the rotational levels due to a permanent dipole moment  $\mu$  are given by<sup>6</sup>

$$\Delta W = \frac{\mu^2 F^2}{hBc} \frac{J(J+1) - 3M^2}{J(J+1)(J-1)(25J+3)}$$

where  $F$  is the amplitude of the low-frequency or dc field.

Figure 2. The Stark shifted rotational energy levels arising from the polarizability anisotropy plotted as a function of  $K = \Delta\alpha \langle \vec{E} \cdot \vec{E} \rangle / (2hBc)$ . Solid lines indicate the energy shifts obtained from the power series approximation and dotted lines show that obtained from numerical calculations.<sup>9</sup> Note that different scales are used for the low-intensity region and the saturated region.

Figure 3. Nonlinear coefficients  $N_2(\eta)$ ,  $N_3(\eta)$ , and  $N_4(\eta)$  and the factor  $\eta Z$  plotted as a function of  $hBc/kT$ .

Figure 4. Saturation of the induced refractive index at low temperatures for a collisionless gas.  $\Delta n = n - n_0$  and  $K$  is the perturbation parameter  $\frac{1}{2} \Delta\alpha \langle \vec{E} \cdot \vec{E} \rangle / hBc$ .

Figure 5. The dependence of the effective factor  $F(T)$  for symmetric top molecules on the ratio of the rotational constants  $A$  and  $B$ . These were evaluated for the high-temperature limit ( $T = 1200^\circ K$ ,  $B = 0.1092 \text{ cm}^{-1}$ ) for which  $F(T)$  depends only on  $A/B$ .



Figure 6. Theoretically predicted time variation of the refractive index change induced by a Gaussian-shaped optical pulse in CS<sub>2</sub> vapor at 296°K. The pulse widths  $\tau$  as defined by Eq. (27) for the individual curve are (a)  $\tau = 5 \times 10^{-12}$  sec. The curves are normalized with respect to  $\Delta n_m = (2\pi N/30n_0) \times \{(\Delta\alpha)^2 A^2/2kT\}$  (which is  $1.74 \times 10^{-10} \text{ A}^2/2 \text{ esu/mole}$ . (b)  $\tau = 1/\pi \times 10^{-12} \text{ sec}$ .

Figure 7. Time evolution for the probability density function  $|\psi|^2$ , (where  $\psi$  is the wave function) of a state that is the superposition of the J=0, M=0 and the J=2, M=0 rotational states of a linear molecule. (a) Polar plot of the rotational wave functions of the ground state and of the excited state with quantum numbers J=2, M=0. The molecular axis is perpendicular to the plane of the paper. (b)-(d) Probability density functions of a superposition state at three moments subsequent to an optical impulse excitation; (b) at  $\omega t = 0$  and  $\omega t = \pi$ ,  $|\psi|^2 = (1/8)(5 - 6 \cos^2\theta + 9 \cos^4\theta)$ , (c) at  $\omega t = \pi/2$ ,  $|\psi|^2 = (1/8)(1 + 6 \cos^2\theta + 9 \cos^4\theta)$ , (d) at  $\omega t = 3\pi/2$ ,  $|\psi|^2 = (1/8)(9 - 18 \cos^2\theta + 9 \cos^4\theta)$ . (e) and (f) Deviation of the probability density functions from that immediately after the excitation at different moments; (e) at  $\omega t = \pi/2$ ,  $\Delta|\psi|^2 = (3 \cos^2\theta - 1)/2$ . (f) at  $\omega t = 3\pi/2$ ,  $\Delta|\psi|^2 = (1 - 3 \cos^2\theta)/2$ . The refractive index change contributed by the superposition state is proportional to  $\Delta|\psi|^2$  at any given time t.

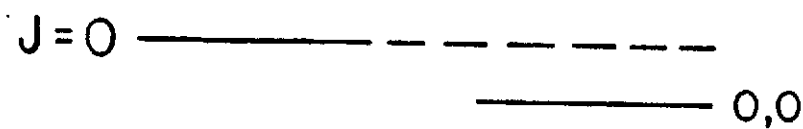
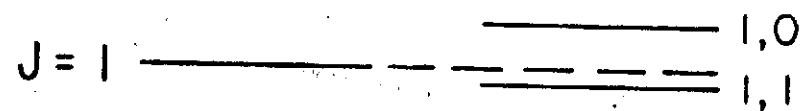
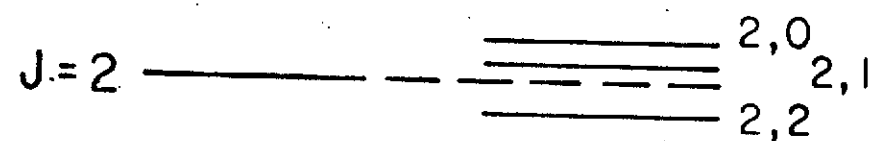
Figure 8. Amplitudes of the coefficient  $T_J$  for CS<sub>2</sub> vapor at 296°K. The curve is normalized with respect to the maximum coefficient  $T_{J_{\max}}$ , where  $J_{\max} = 42$ .

Figure 9. Normalized peak amplitudes of the refractive index  $\Delta n_p$  of the refractive index burst for a time delay  $1/4 Bc$  after excitation for  $CS_2$  vapor at  $296^\circ K$  as a function of the excitation pulse width (defined by Eq. (24)). The normalization is as for Fig. 6.

Figure 10. Theoretically predicted refractive index bursts induced by Gaussian-shaped optical pulses. (a) Bursts in  $CS_2$  vapor at  $296^\circ K$ . The normalization is as for Fig. 6. The excitation pulse widths are (I)  $\tau = 0.2 \times 10^{-12}$  sec, (II)  $\tau = 0.8 \times 10^{-12}$  sec, and (III)  $\tau = 2 \times 10^{-12}$  sec, (b) Bursts in  $CH_3Cl$  vapor at  $296^\circ K$ . The normalization constant is  $\Delta n_s = F(T) (2\pi N / 30n_o) [(\Delta\alpha)^2 A^2 / 2kT]$  where  $F(T) = 0.843$  (equal to  $4.27 \times 10^{-12} A^2 / 2$  esu/mole). The excitation pulse widths are (I)  $\tau = 0.1 \times 10^{-12}$  sec, (II)  $\tau = 0.37 \times 10^{-12}$  sec, and (III)  $\tau = 10^{-12}$  sec.

Figure 11. Illustration of refractive index bursts induced by an optical pulse whose intensity is not symmetric about any time.  $CS_2$  at  $296^\circ K$  has been assumed;  $\Delta n_m$  is the same as for Fig. 6 but with  $A^2 = C_2^2$ . (I) The contribution to the burst by the portion of the optical pulse that is an even function of time (Eq. (29c)). (II) The contribution due to the portion that is an odd function of time (Eq. (29b) with  $C_1 = 0.4C_2$ ), and (III) the total theoretically predicted burst.

# PERMANENT DIPOLE



# INDUCED DIPOLE

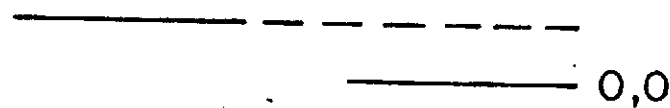
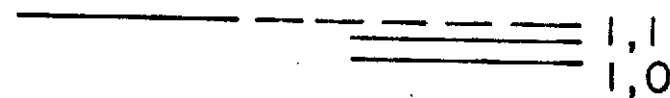
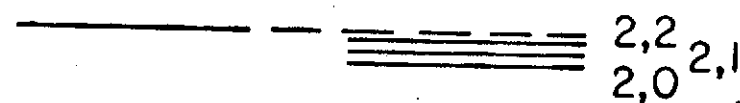


Fig. 1

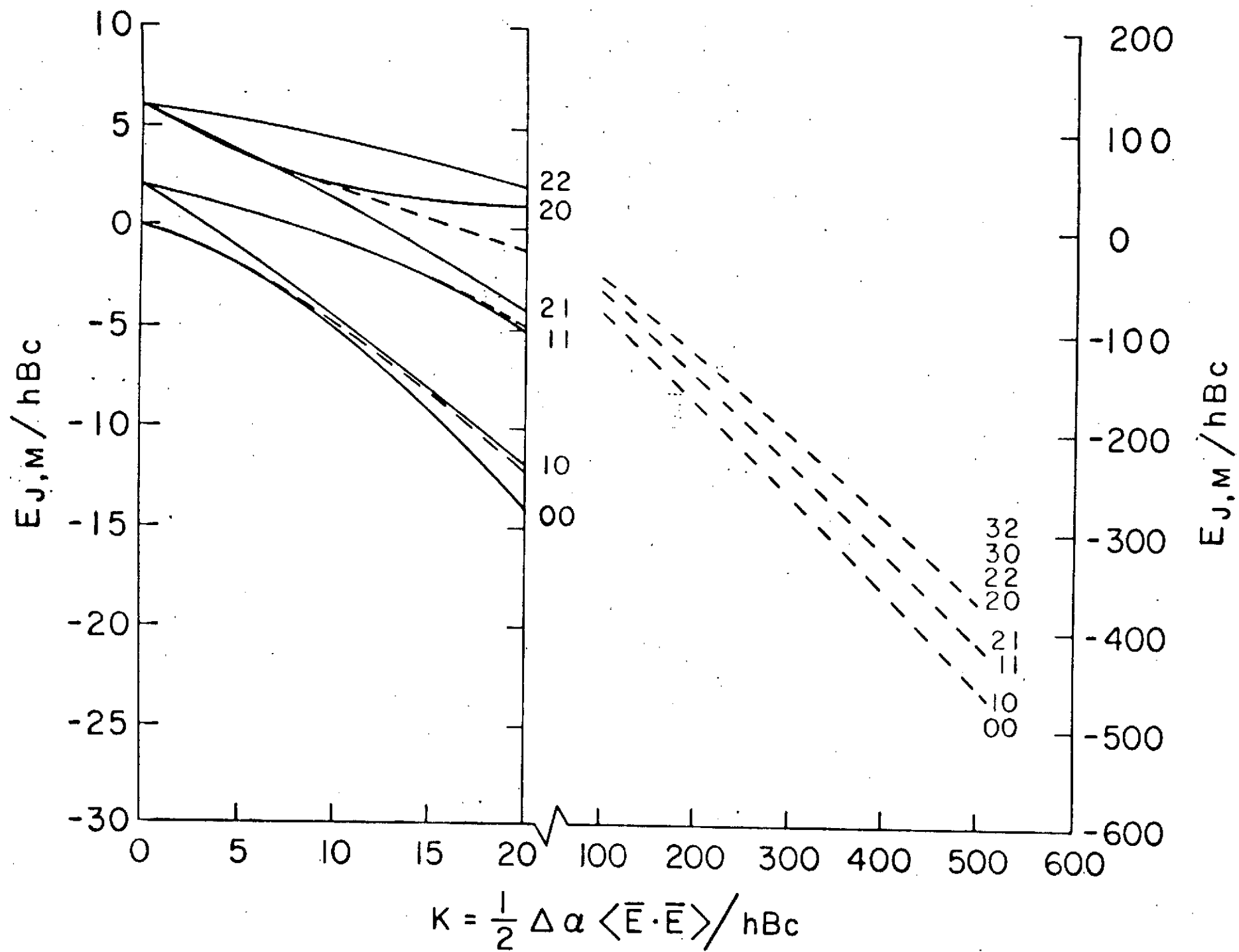


Fig. 2

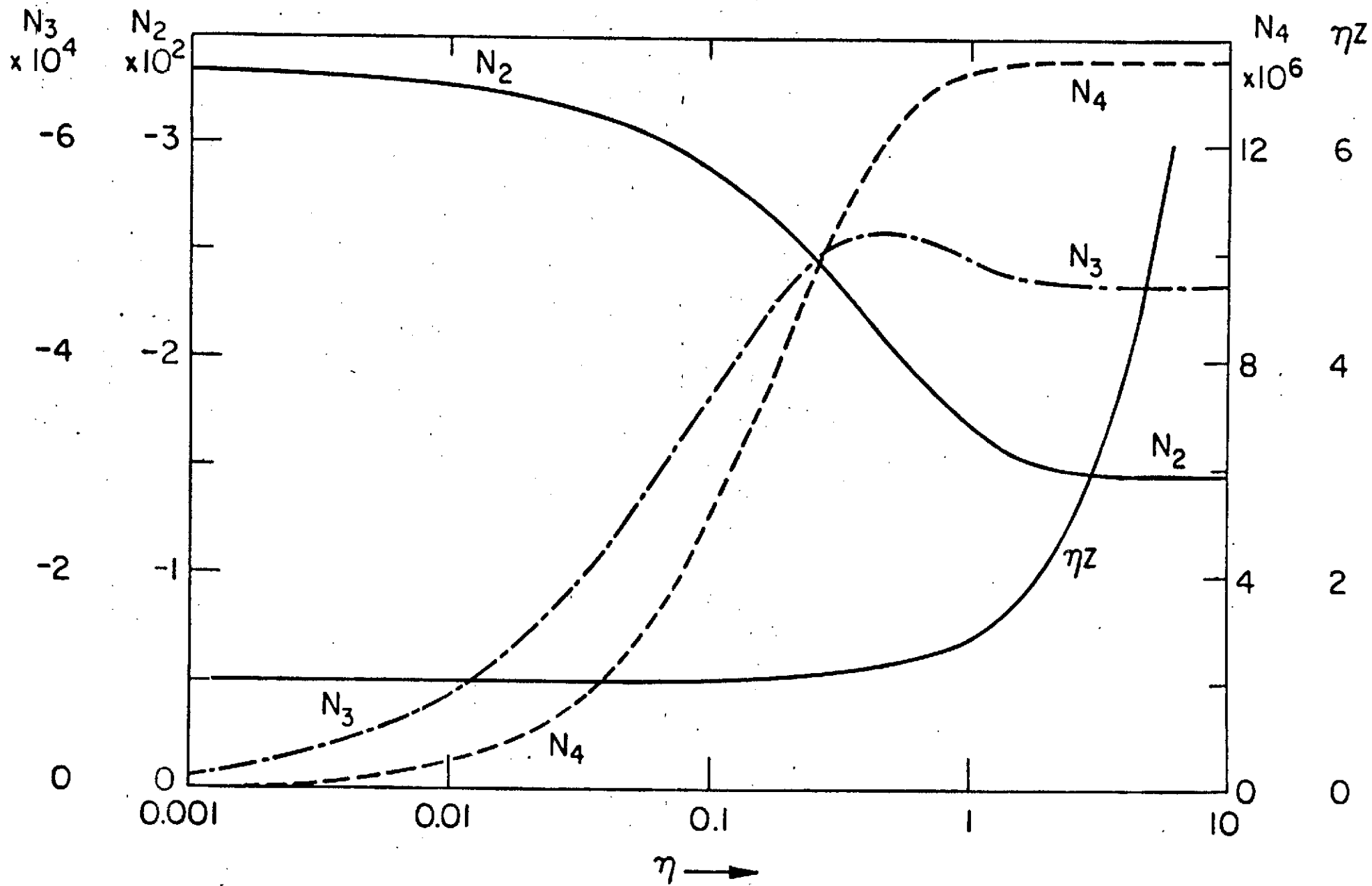


Fig. 3

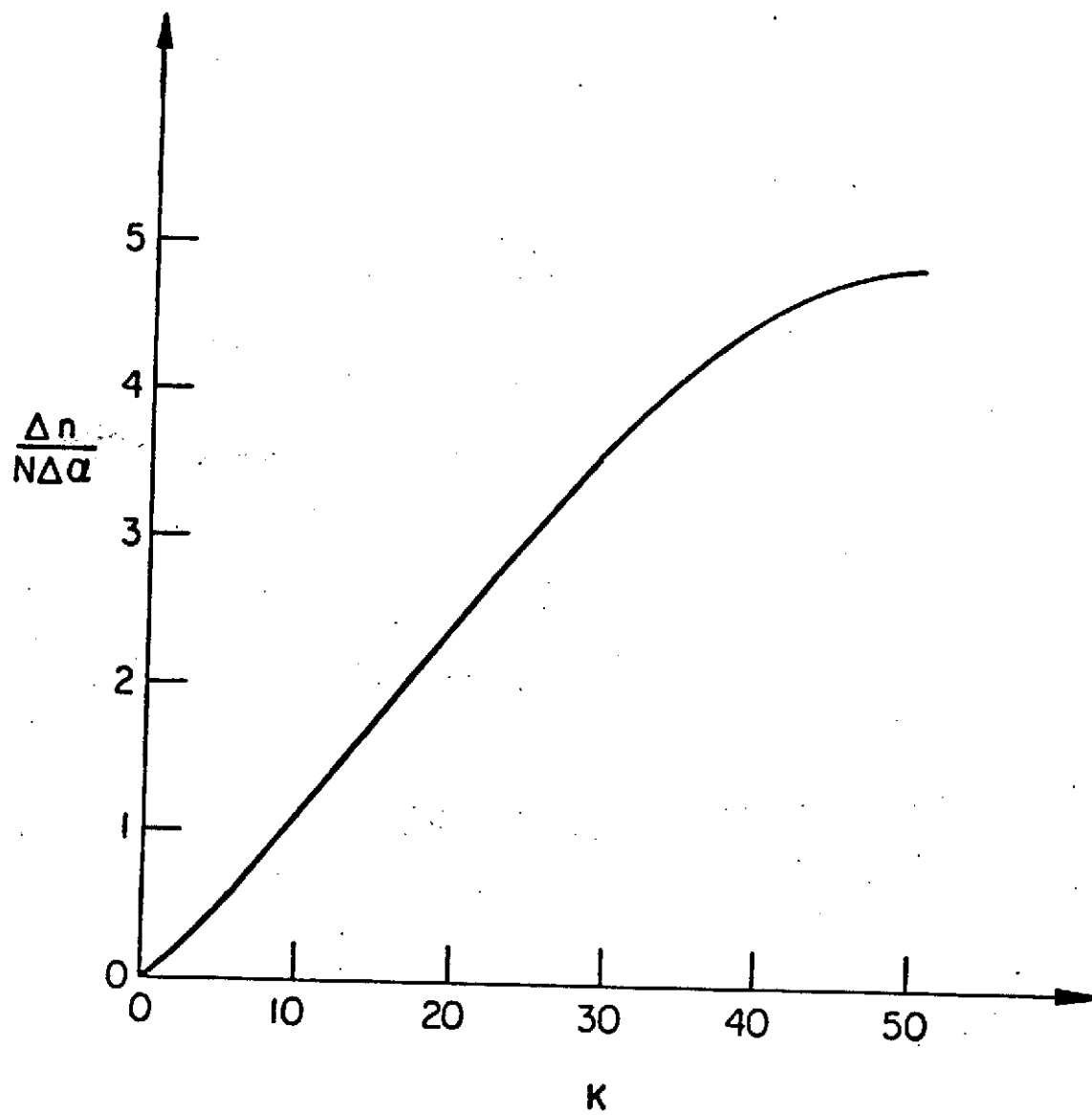


FIGURE 4

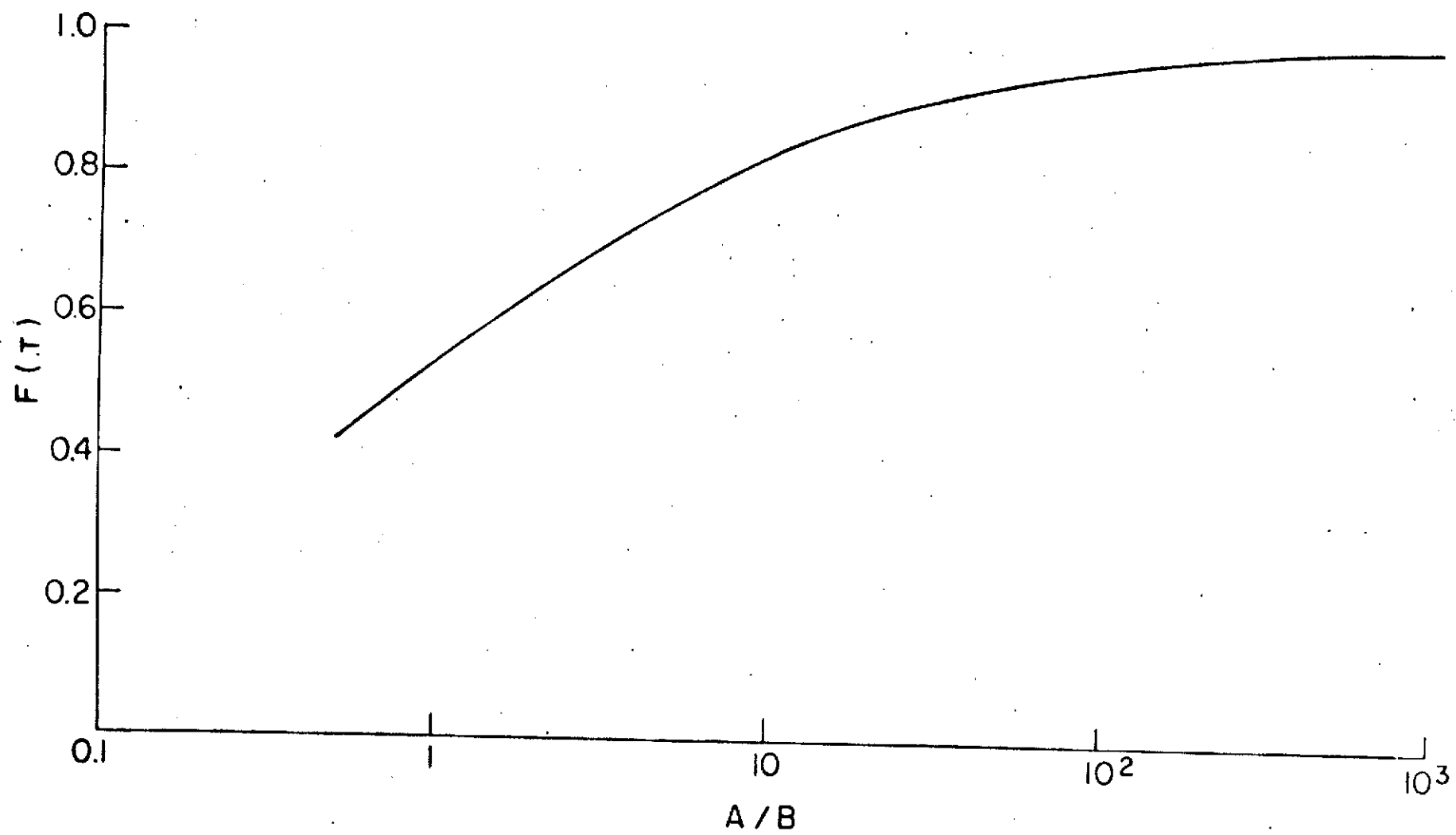


Fig. 5

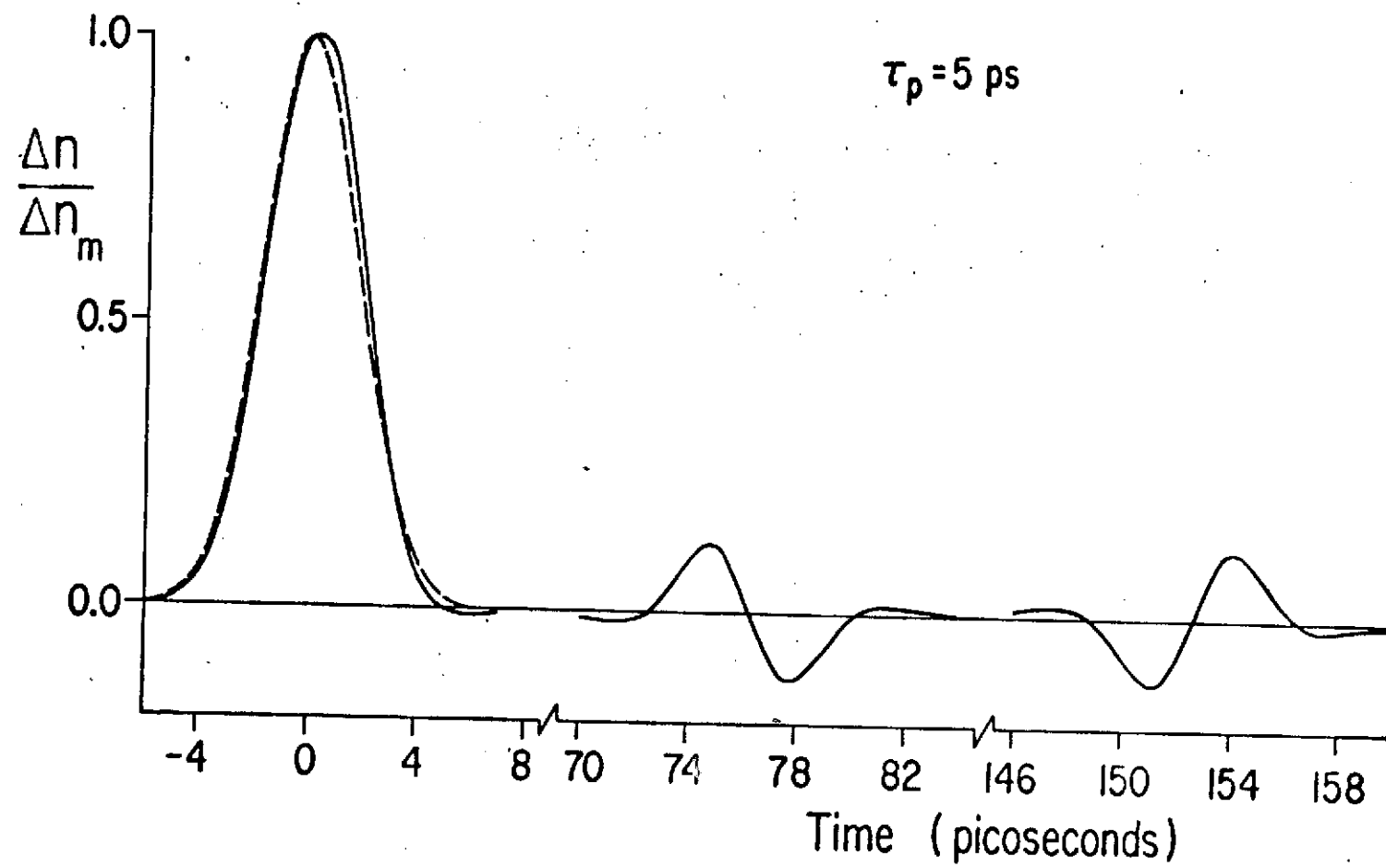


FIGURE 6a



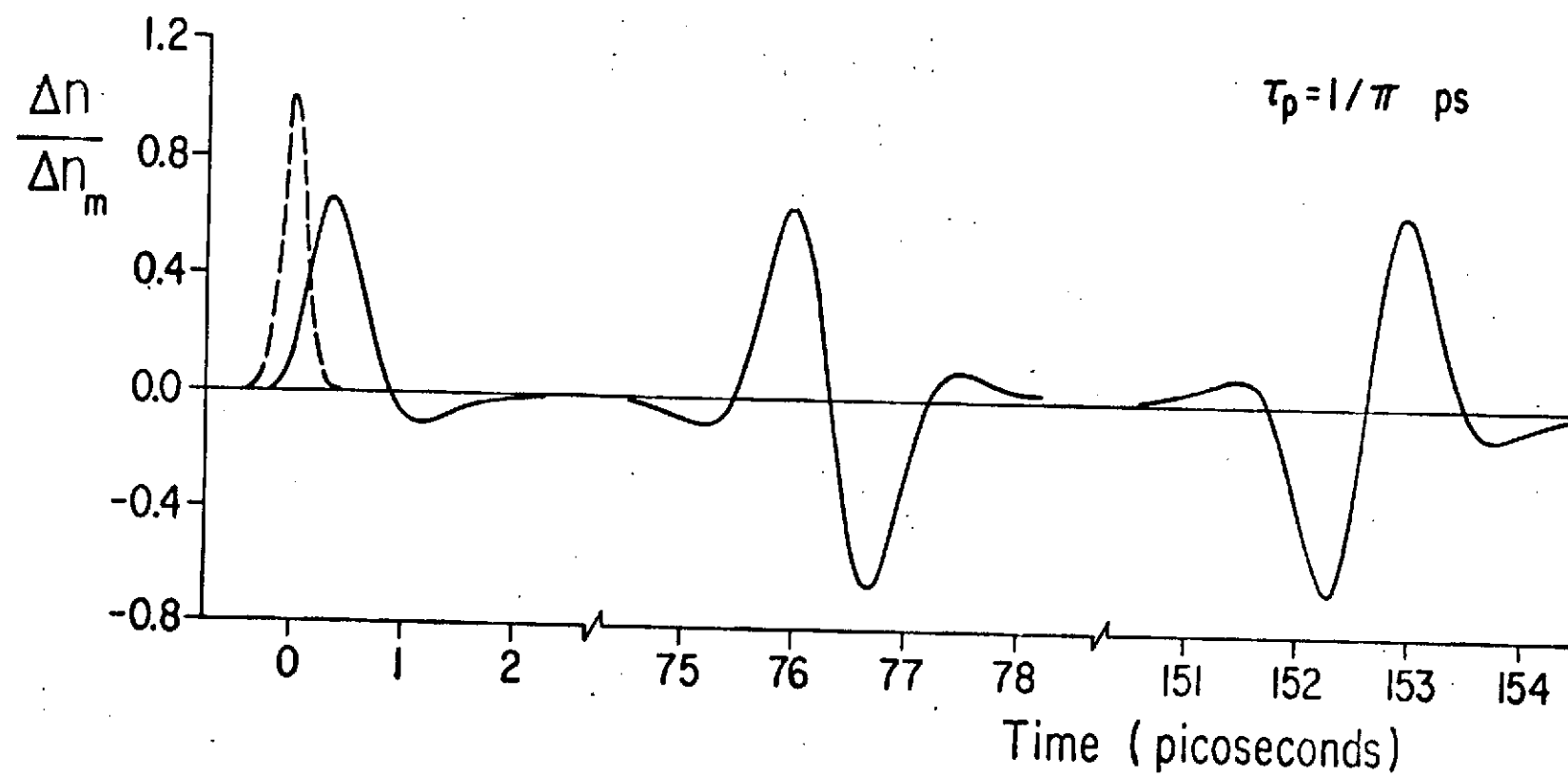
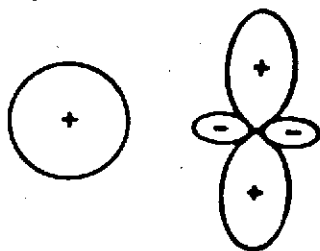
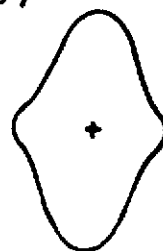


FIGURE 6b

(a)



(b)



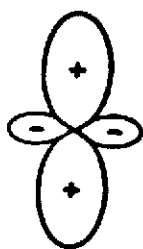
(c)



(d)



(e)



(f)

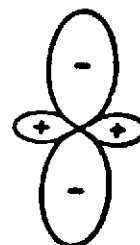


FIGURE 7

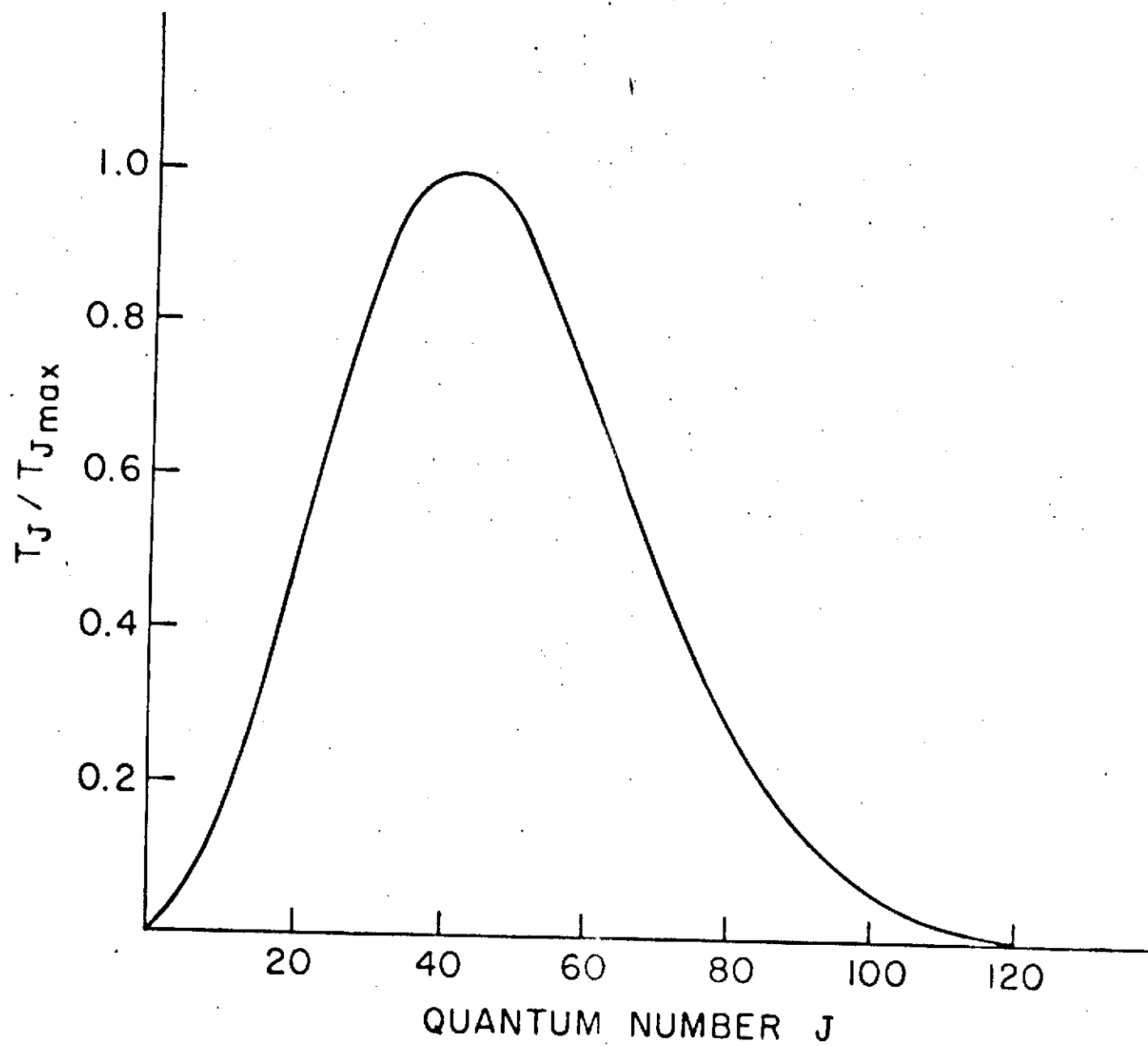


Fig. 8

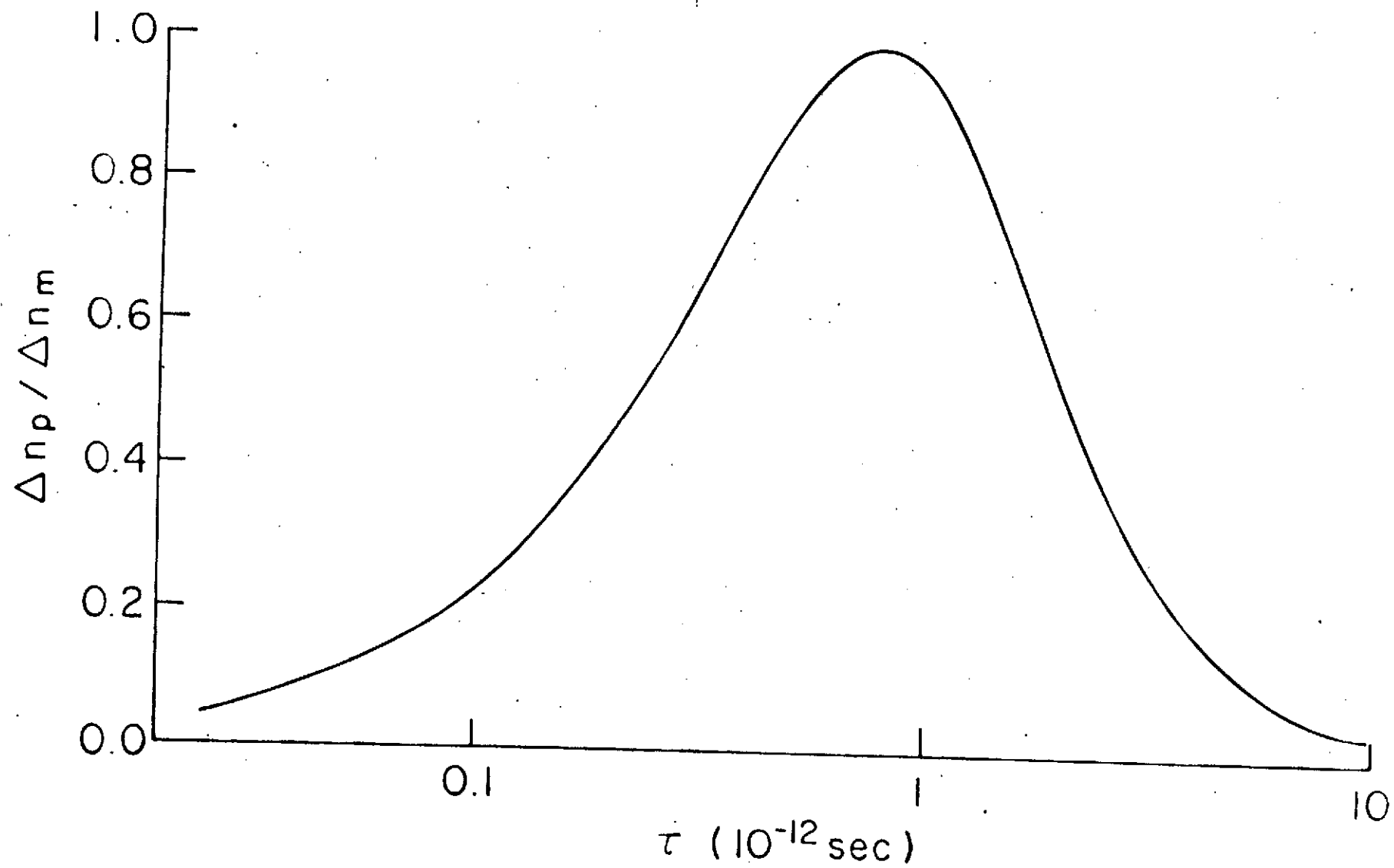


Fig. 9

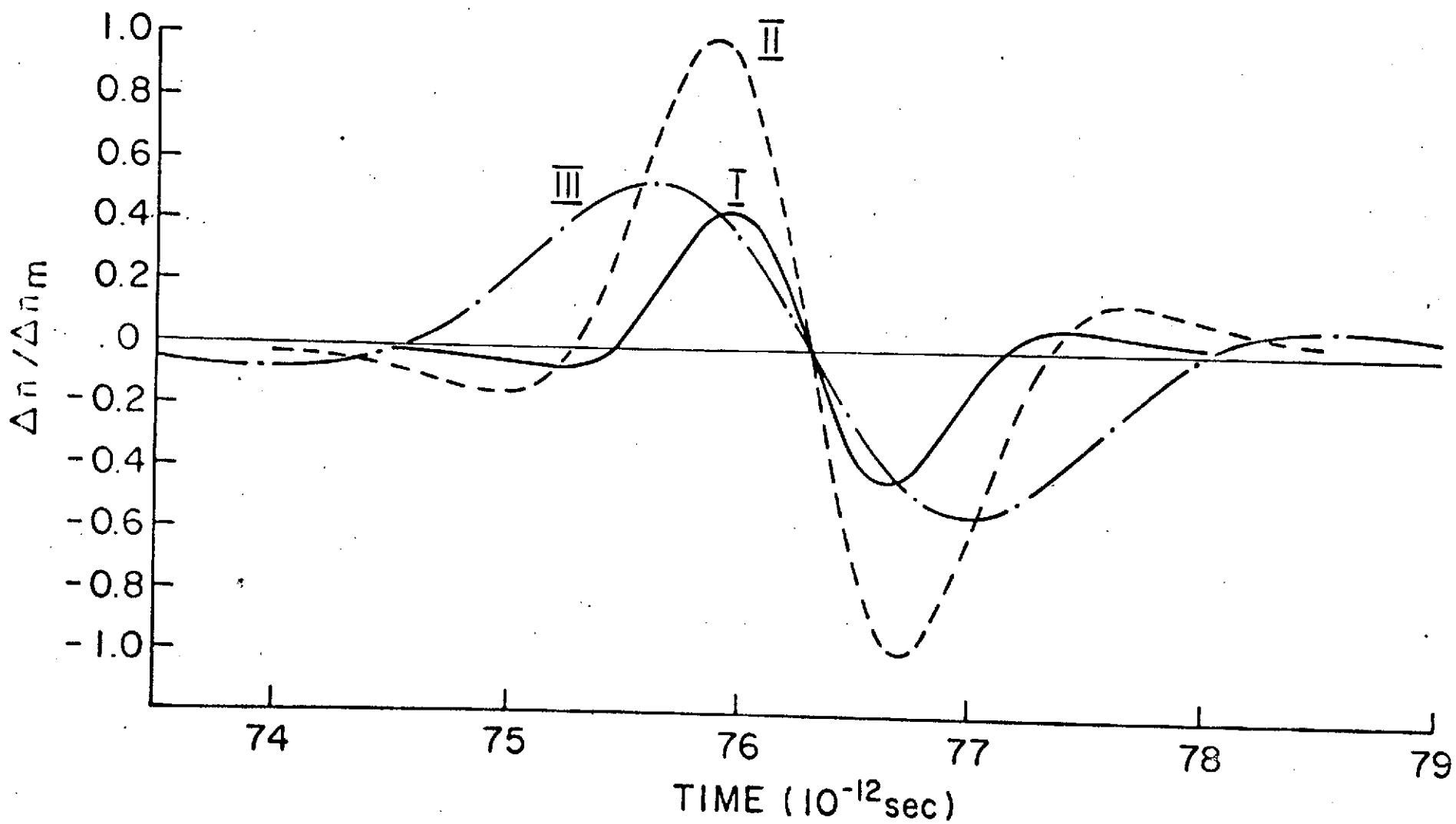


Fig. 10a

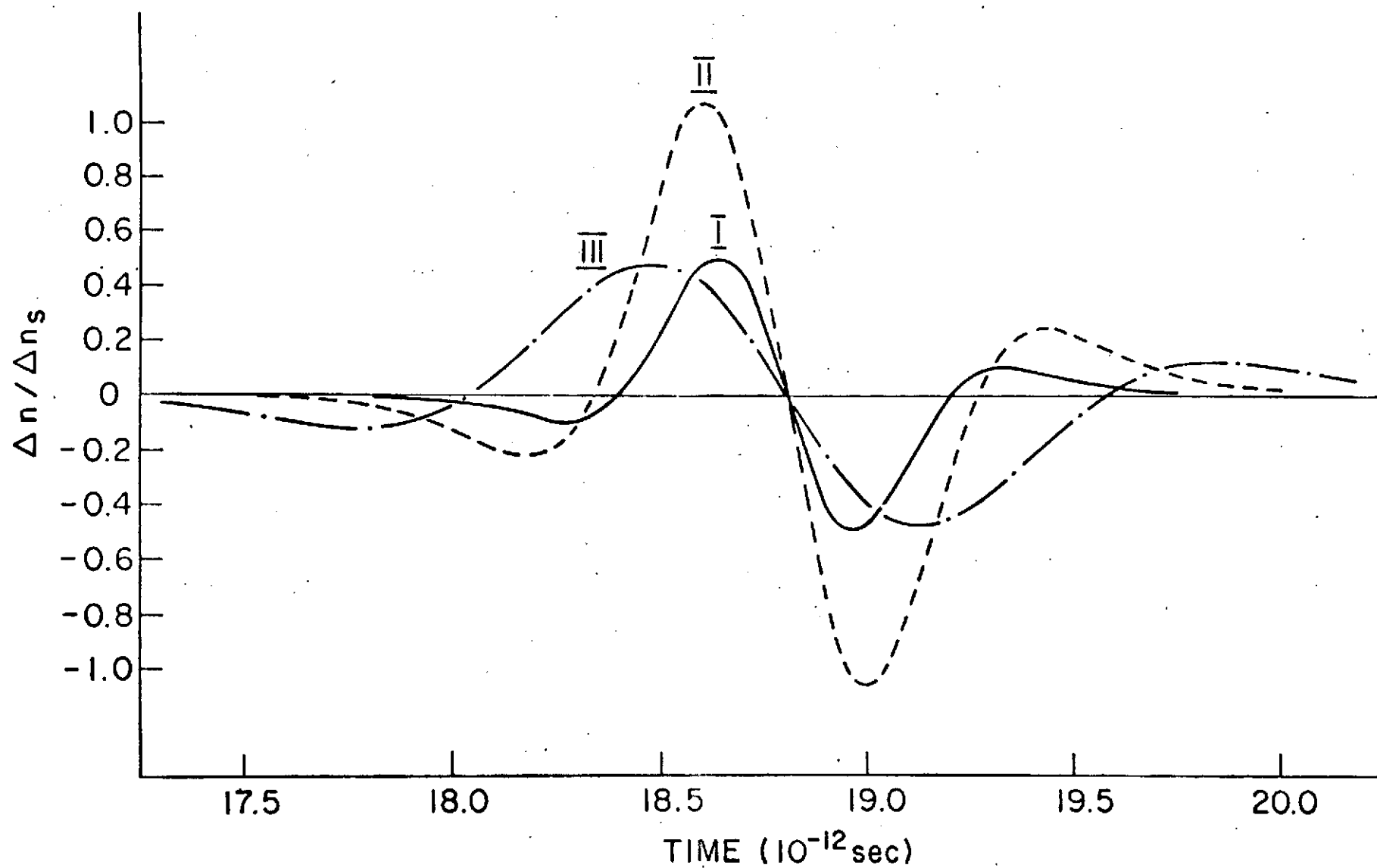


Fig. 10b

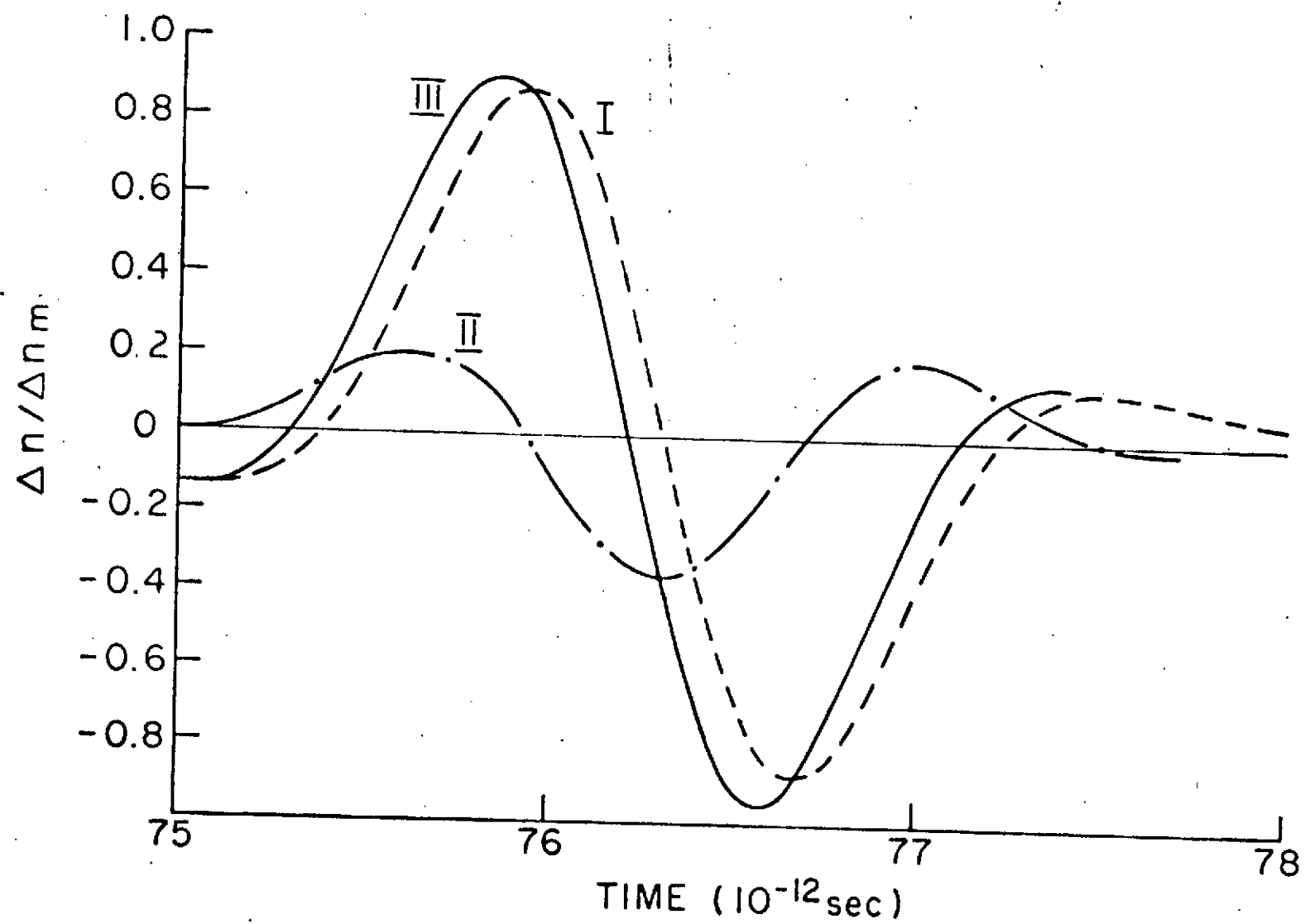


Fig. 11